



SpaceSUITE



UNIVERSITAT POLITÈCNICA DE CATALUNYA
BARCELONATECH
Departament de Teoria del Senyal
i Comunicacions

IEEC
Institut d'Estudis
Espacials de Catalunya

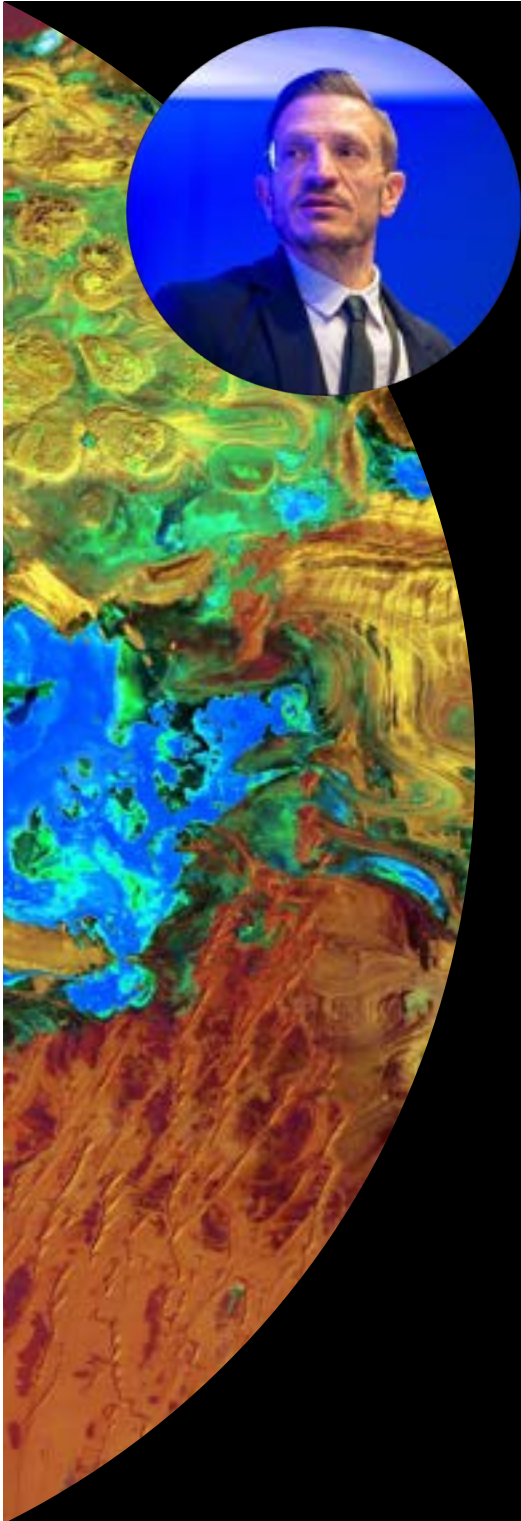
Target Decomposition Theorems & Thematic Classification for SAR Polarimetry

Carlos López-Martínez

Int. School on on PoSAR
Dec. 2024
Stirling, Scotland

Universitat Politècnica de Catalunya – UPC
Signal Theory and Communications Department – TSC
Institute of Space Studies of Catalonia - IEEC
carlos.lopezmartinez@upc.edu

Co-funded by the European Union. Views and opinions expressed are however those of the author(s) only and do not necessarily reflect those of the European Union or the European Education and Culture Executive Agency (EACEA). Neither the European Union nor EACEA can be held responsible for them.



Carlos LÓPEZ-MARTÍNEZ, PhD
Scientist | Engineer | Associate Professor



UNIVERSITAT POLITÈCNICA DE CATALUNYA
BARCELONATECH

Departament de Teoria del Senyal
i Comunicacions



Technical University of Catalonia UPC
Signal Theory and Communications Department TSC
Remote Sensing Lab. (RsLAB)

Institute of Space Studies of Catalonia IEEC

📞 +34 93 401 6785

✉ carlos.lopezmartinez@upc.edu

🌐 carloslopezmartinez.info

linkedin.com/in/clopmar

- Multidimensional SAR Systems
- Polarimetric Incoherent Decompositions
 - Model based decompositions
 - Mathematical based decompositions
 - Speckle noise effects
- Forestry Applications
 - Thematic Classification
 - Forest Fires & Change Detection

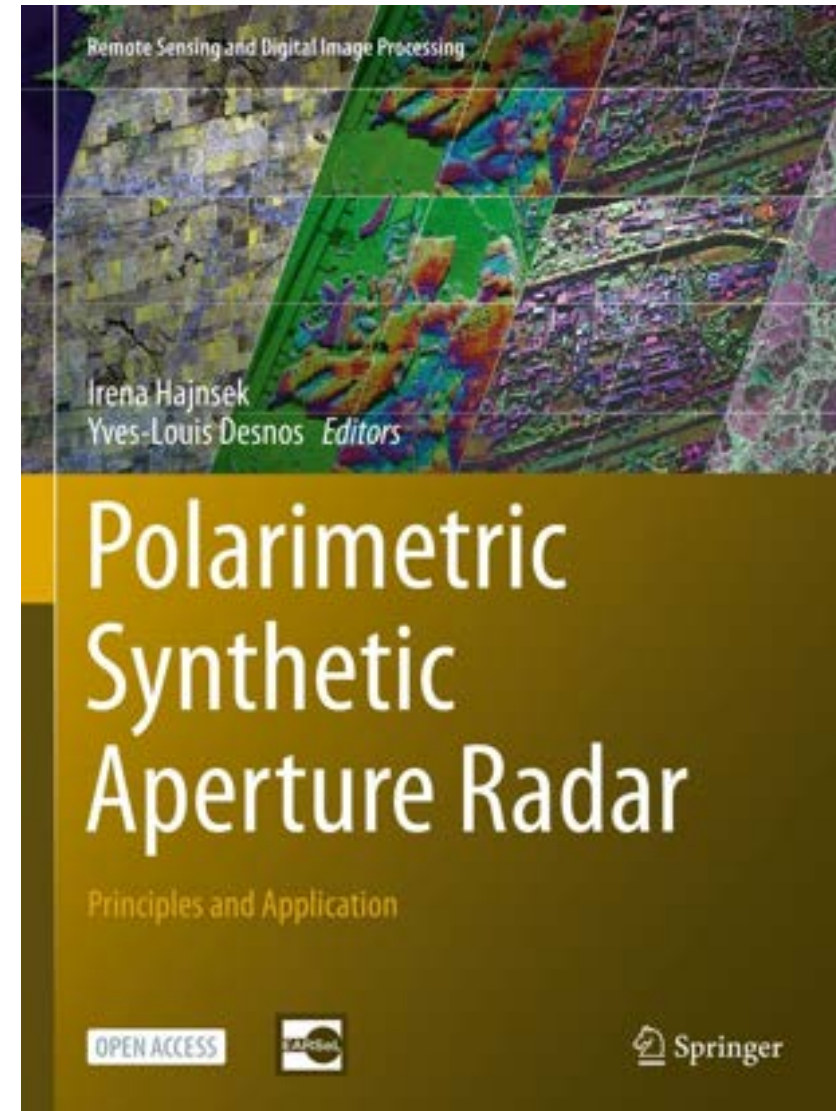
Polarimetric Synthetic Aperture Radar Principles and Application

Chapter 1

Basic Principles of SAR Polarimetry

C. López-Martínez, E. Pottier

Open Access Book
<https://bit.ly/3O7I3gh>



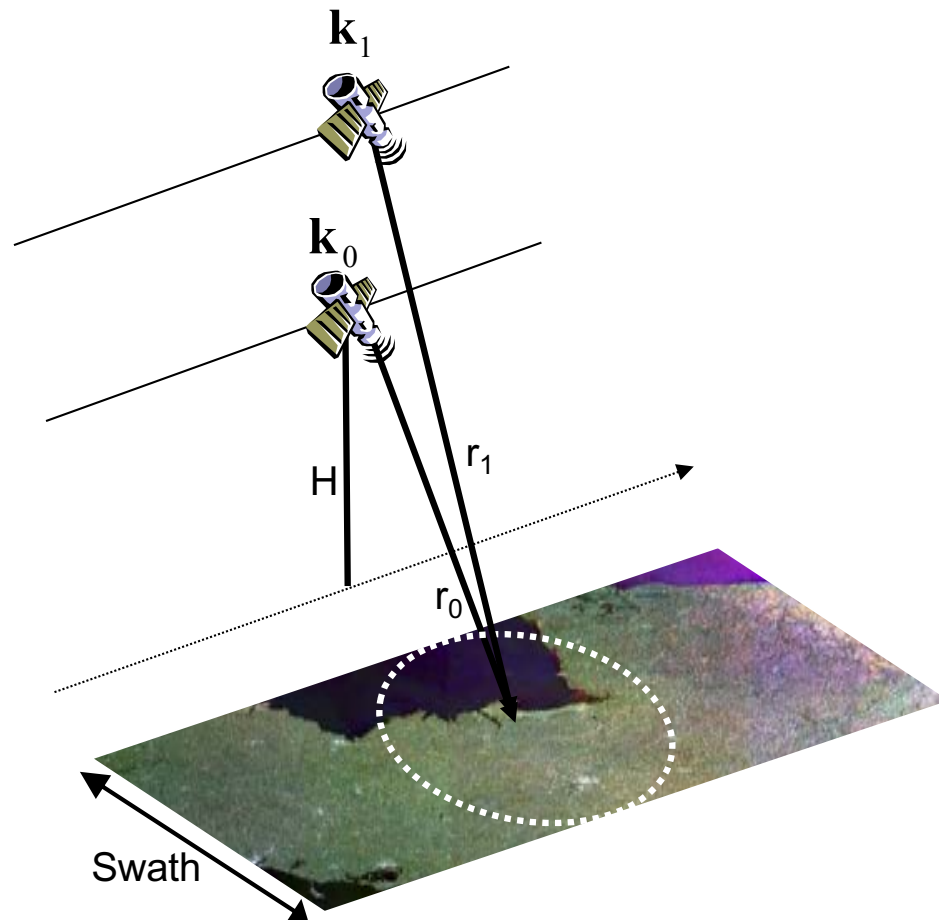


Multidimensional SAR Systems

Multidimensional SAR Systems

The multidimensional SAR system acquires m complex SAR images

Target vector $\mathbf{k} = [S_1, S_2, \dots, S_m]^T$



The properties of the target vector follow from the properties of a single SAR image

- \mathbf{k} is deterministic for point scatterers. It contains all the necessary information to characterize the scatterer
- \mathbf{k} is a multidimensional random variable for distributed scatterers due to speckle. A single sample does not characterize the scatterer

SAR images characterized through second order moments

- Second order moments in multidimensional SAR data are matrix quantities

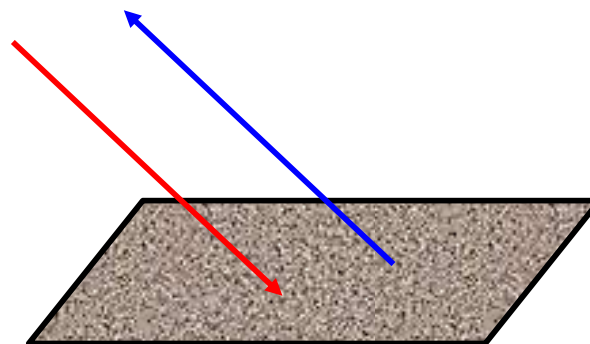
Multidimensional SAR Systems

- SAR Interferometry (InSAR): $m=2$. Topographic information
- Differential SAR interferometry (DInSAR): $m=3$. Topographic changes information
- SAR Polarimetry (PolSAR): $m=3,4$. Geometric characterization and classification of the scatterers being imaged
- Polarimetric SAR interferometry (PolInSAR): $m=6,8$. Study and characterization of volumetric structures
- SAR Tomography/Multibaseline: $m>2$. Vertical profiling
- Multitemporal SAR: $m>2$. Change detection and temporal analysis
- Multifrequency SAR: $m>2$. Characterization of the scatters being imaged

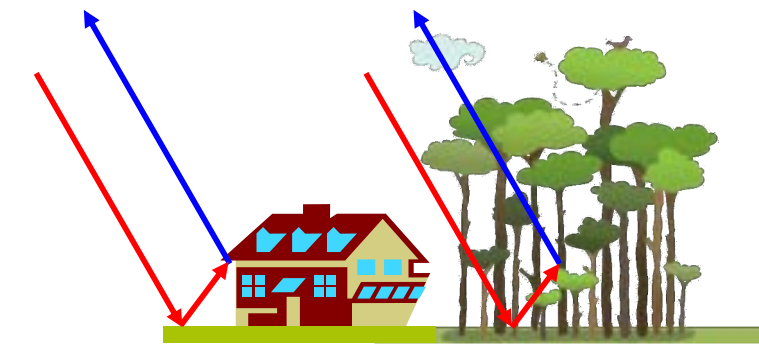
SAR Polarimetry

Physical interpretation of the Pauli components

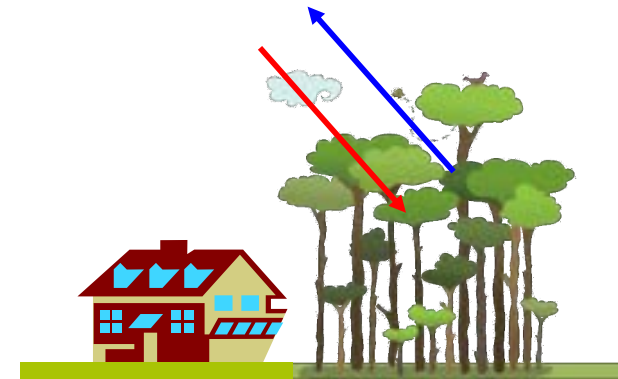
- $|S_{hh} + S_{vv}|^2$ is related to **single bounce scattering**, for example, a rough surface



- $|S_{hh} - S_{vv}|^2$ is related to **double bounce scattering**

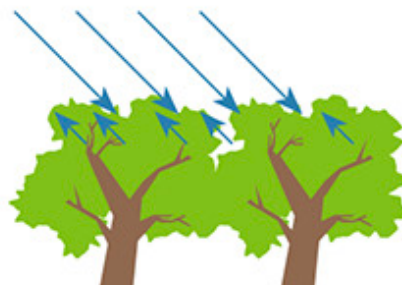


- $|S_{hv}|^2$ is related to **volume scattering**

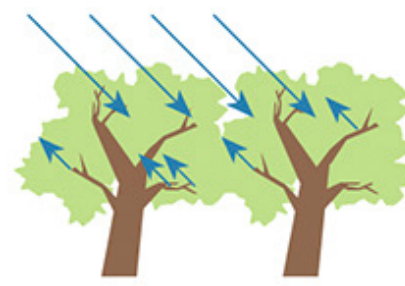


Multifrequency SAR

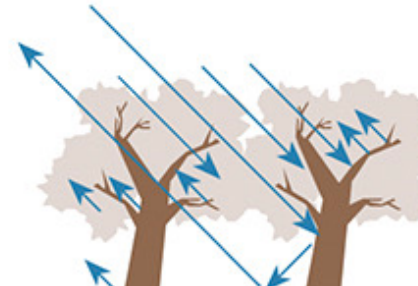
Microwave radiation (1 to 10 GHz) penetrate semi-transparent media, so **SAR data is sensitive to the vegetation canopy structure** depending on the carrier frequency



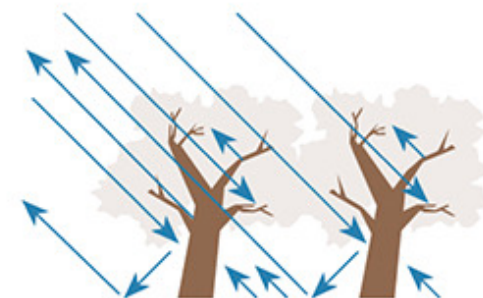
X-BAND 3 cm



C-BAND 6 cm



L-BAND 24 cm



P-BAND 65 cm

Penetration capability depends also on the **incidence angle**



Polarimetric Decompositions

Polarimetric Target Decompositions Theorems allow the interpretation of measured PolSAR data by decomposing them

■ Coherent Decompositions

- Applied to the first order descriptors, i.e., the Scattering Matrix
- Valid for the interpretation of Pure or Deterministic scatters
- Decomposition of the data into canonical scattering mechanisms

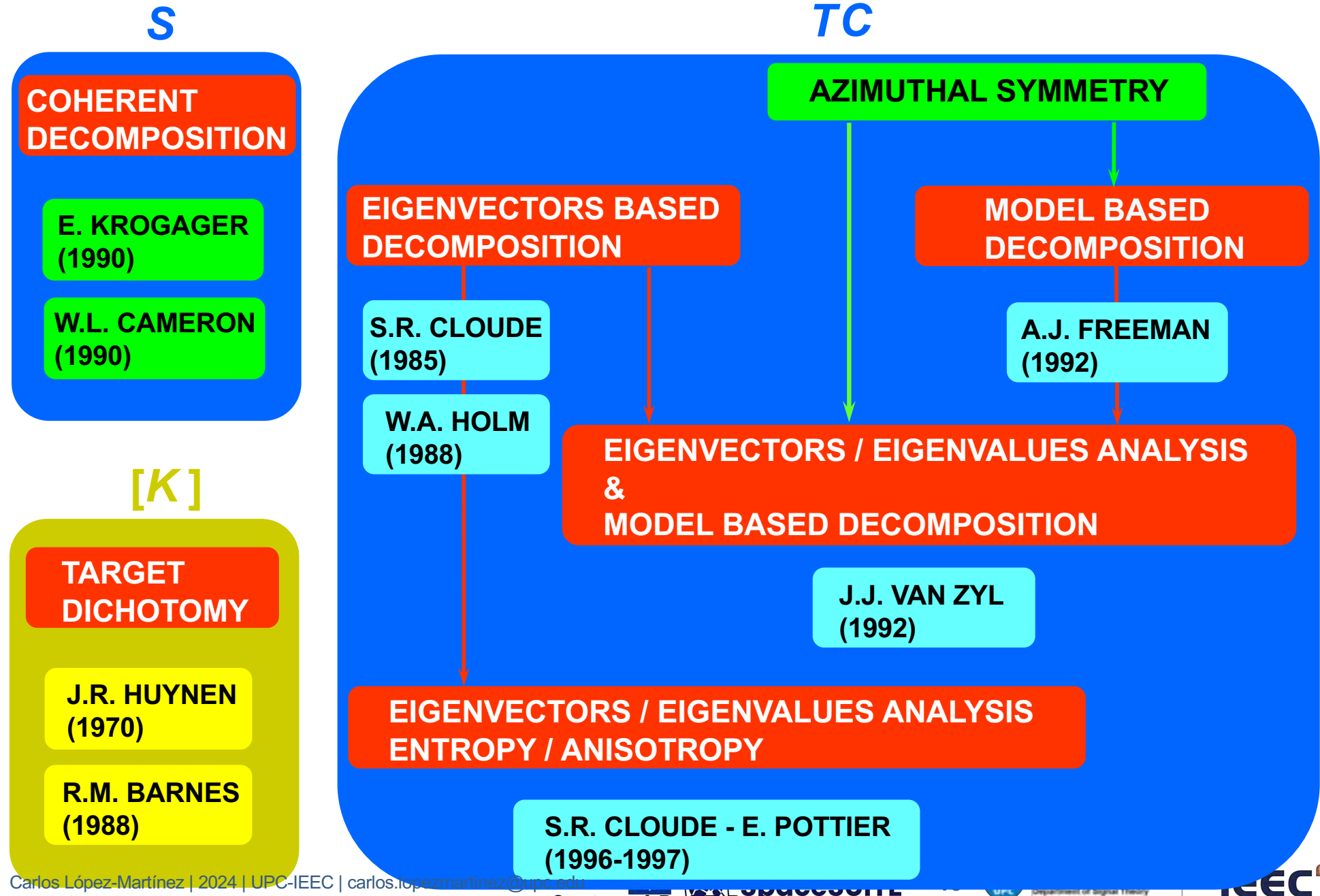
$$\mathbf{S} = \sum_{i=1}^k c_i \mathbf{S}_i$$

■ Incoherent Decompositions

- Applied to second order descriptors, i.e., the Covariance and Coherency matrices
- Valid for the interpretation of Deterministic and Distributed scatters
- Decomposition of the data into simple scattering mechanisms that may, or not, admit an equivalent scattering matrix

$$\langle \mathbf{C} \rangle = \sum_{i=1}^k c_i \mathbf{C}_i \quad \langle \mathbf{T} \rangle = \sum_{i=1}^k c_i \mathbf{T}_i$$

Target Decomposition Theorems



Eigenvalue/vectors Decomposition

Decomposition proposed by Shane Cloude, based on the mathematical decomposition of the coherency matrix on its **eigenvalue and eigenvectors**

$$\mathbf{k}_p = \frac{1}{\sqrt{2}} \begin{bmatrix} S_{hh} + S_{vv} \\ S_{hh} - S_{vv} \\ 2S_{hv} \end{bmatrix}$$

Sample

$$\langle \mathbf{T} \rangle = \frac{1}{N} \sum_{i=1}^N \mathbf{k}_i \mathbf{k}_i^H = \frac{1}{N} \sum_{i=1}^N \mathbf{T}_i$$

Estimation of the covariance matrix

■ Decomposition (i)

$$\langle \mathbf{T} \rangle = \mathbf{U} \boldsymbol{\Sigma} \mathbf{U}^{-1} = \begin{bmatrix} \mathbf{u}_1 & \mathbf{u}_2 & \mathbf{u}_3 \end{bmatrix} \begin{bmatrix} \lambda_1 & 0 & 0 \\ 0 & \lambda_2 & 0 \\ 0 & 0 & \lambda_3 \end{bmatrix} \begin{bmatrix} \mathbf{u}_1 & \mathbf{u}_2 & \mathbf{u}_3 \end{bmatrix}^H$$

- The eigenvectors \mathbf{u}_1 , \mathbf{u}_2 and \mathbf{u}_3 are orthonormal
- The eigenvalues are real $\lambda_1 > \lambda_2 > \lambda_3 \geq 0$

H/A/ α Decomposition

Original Eigenvalue/Eigenvector decomposition

$$\langle \mathbf{T} \rangle = \mathbf{U} \boldsymbol{\Sigma} \mathbf{U}^{-1} = \begin{bmatrix} & & \\ \mathbf{u}_1 & \mathbf{u}_2 & \mathbf{u}_3 \\ & & \end{bmatrix} \begin{bmatrix} \lambda_1 & 0 & 0 \\ 0 & \lambda_2 & 0 \\ 0 & 0 & \lambda_3 \end{bmatrix} \begin{bmatrix} & & \\ \mathbf{u}_1 & \mathbf{u}_2 & \mathbf{u}_3 \\ & & \end{bmatrix}^H$$

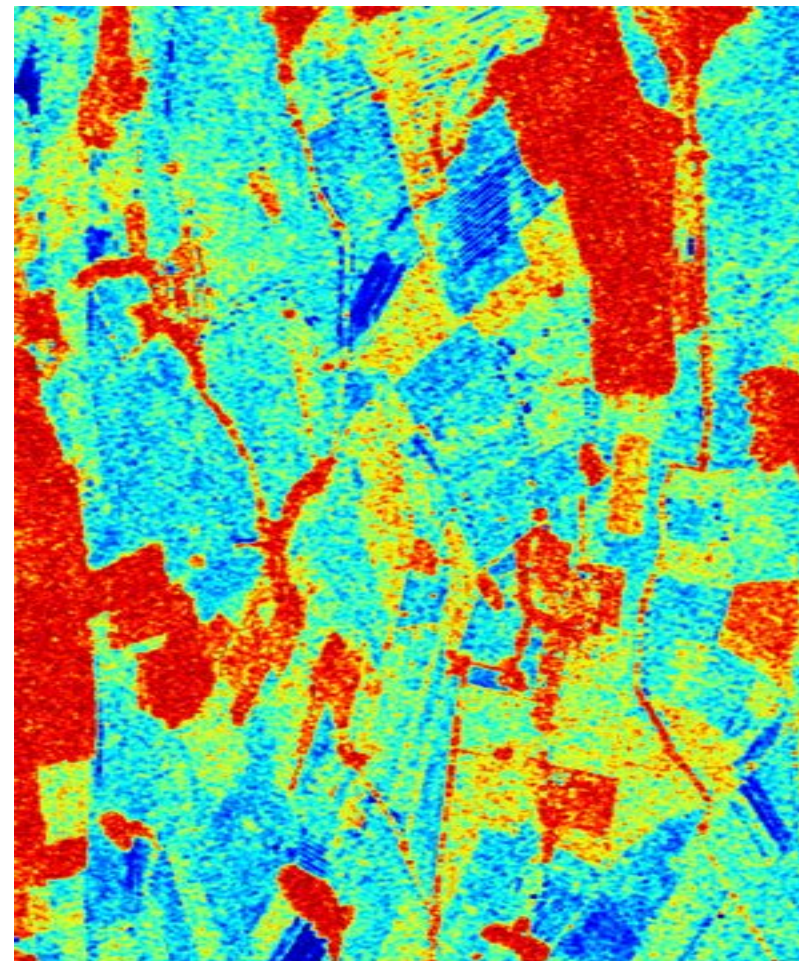
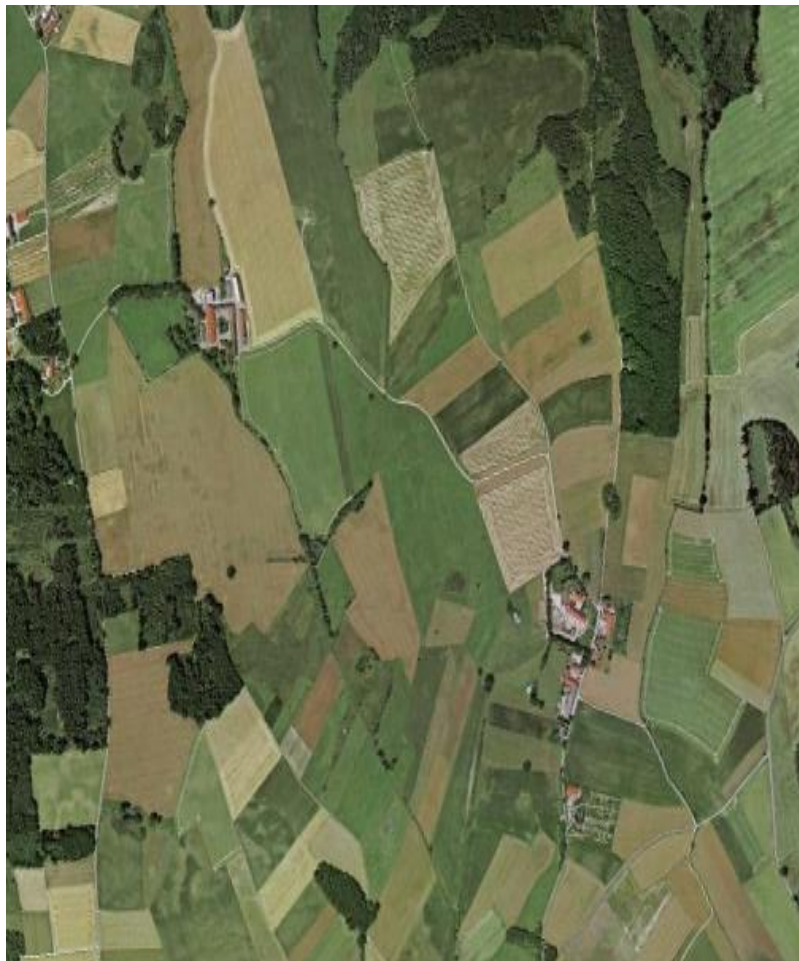


H/A/ α decomposition allows a physical interpretation

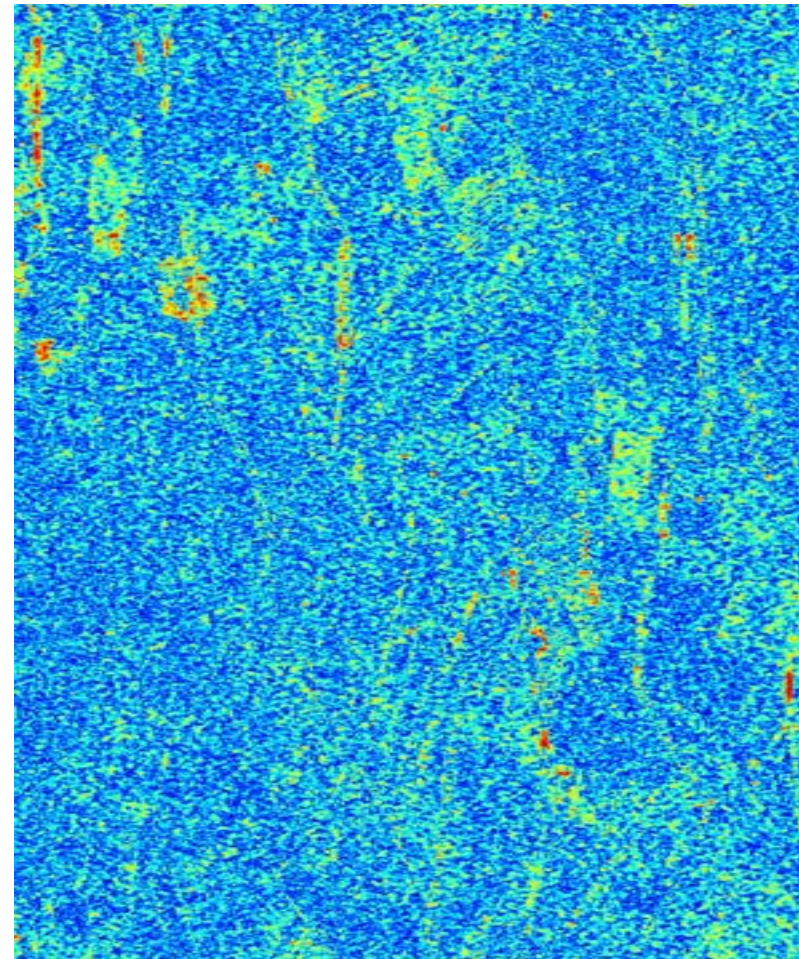
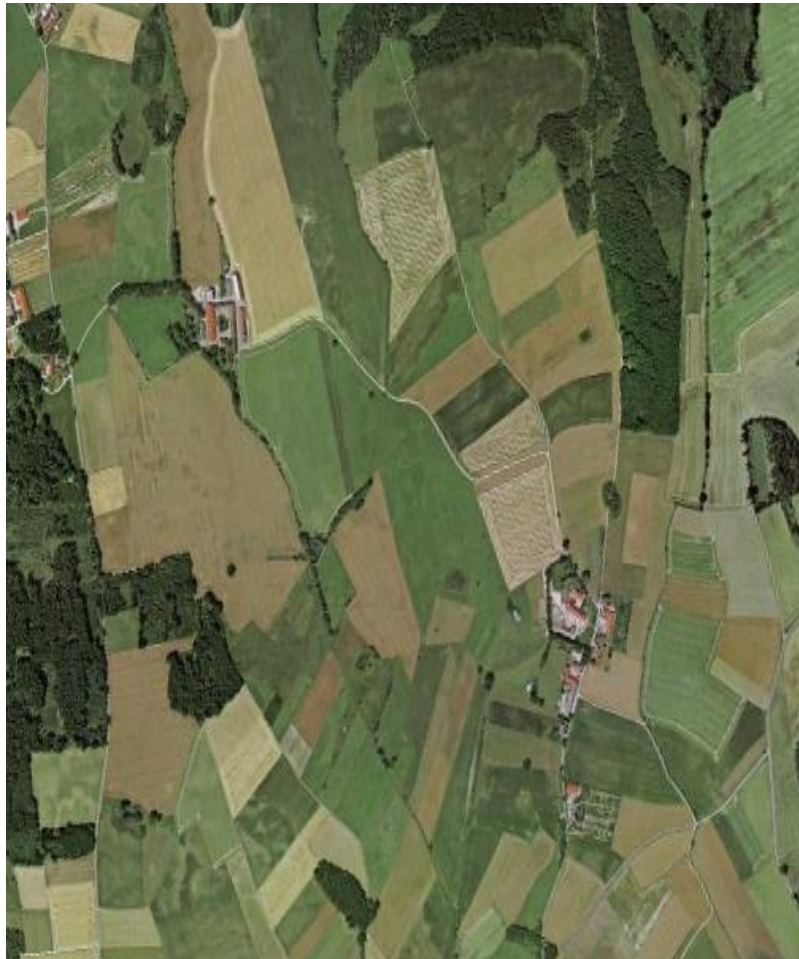
$$H = -\sum_{i=1}^3 P_i \log_3(P_i) \quad A = \frac{\lambda_2 - \lambda_3}{\lambda_2 + \lambda_3}$$

$$\underline{\alpha}$$

H/A/ α Decomposition



H/A/ α Decomposition

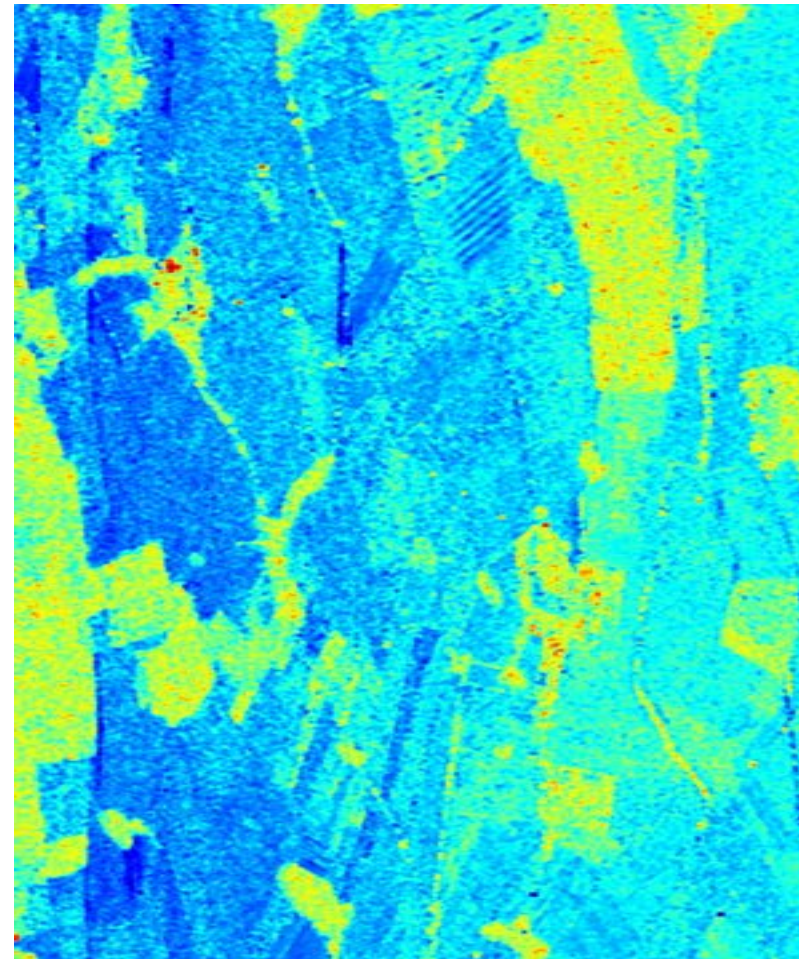
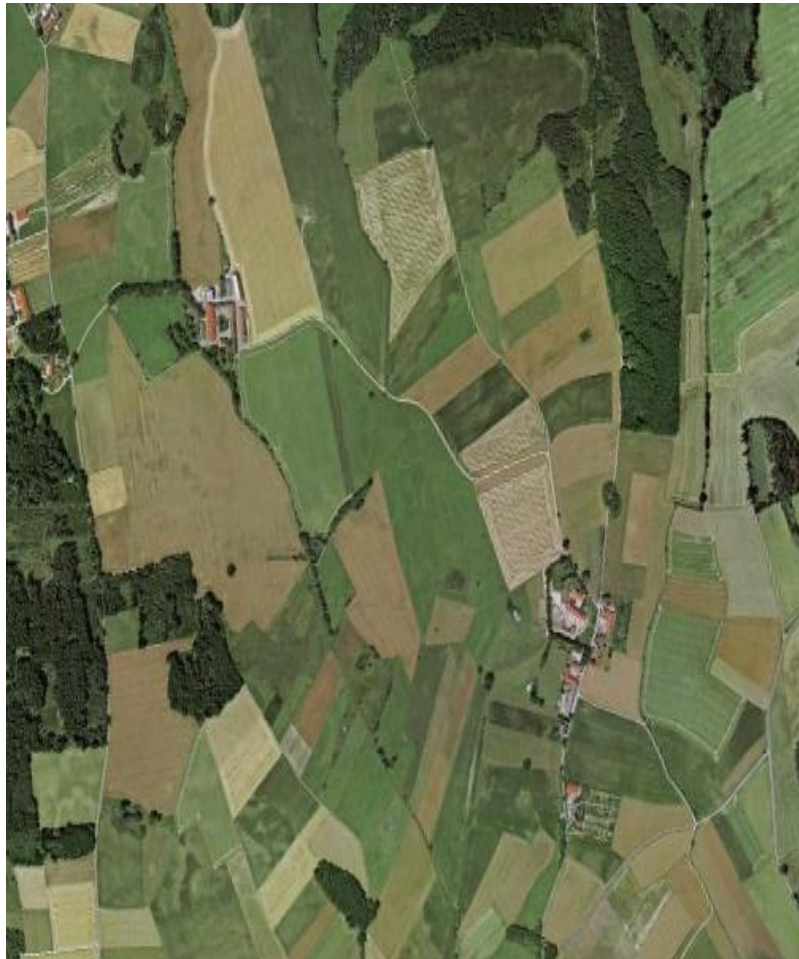


0

0.5

1.0

H/A/ α Decomposition



Alpha (α)

H/A/α Decomposition

A rotation about the line of sight is a **unitary transformation**

Rotation about the line-of-sight

$$\langle \mathbf{T}(\theta) \rangle = \mathbf{R}(\theta) \langle \mathbf{T} \rangle \mathbf{R}^{-1}(\theta) = \mathbf{R}(\theta) \mathbf{U} \Sigma \mathbf{U}^H \mathbf{R}^{-1}(\theta) = \mathbf{U}' \Sigma \mathbf{U}'^H$$

$$\mathbf{R}(\theta) = \begin{bmatrix} 1 & 0 & 0 \\ 0 & \cos(2\theta) & \sin(2\theta) \\ 0 & -\sin(2\theta) & \cos(2\theta) \end{bmatrix}$$

$$\langle \mathbf{T} \rangle = \mathbf{U} \Sigma \mathbf{U}^{-1} = \begin{bmatrix} \mathbf{u}_1 & \mathbf{u}_2 & \mathbf{u}_3 \end{bmatrix} \begin{bmatrix} \lambda_1 & 0 & 0 \\ 0 & \lambda_2 & 0 \\ 0 & 0 & \lambda_3 \end{bmatrix} \begin{bmatrix} \mathbf{u}_1 & \mathbf{u}_2 & \mathbf{u}_3 \end{bmatrix}^H$$

- **Eigenvalues** are roll-invariant, i.e., not affected by a rotation
- **Probabilities** are roll-invariant
- **Average alpha angle** is roll-invariant

H/A/ α Decomposition

Interest of Multidimensional SAR imagery → QUANTITATIVE REMOTE SENSING



Determined by the capacity to reduce Speckle noise, i.e., the capacity to estimate correctly the Bio- and Geophysical parameters



Speckle noise reduction

Low averaging level

- Problem not considered

High averaging level

- Brute force method
- Information mixture
- Spatial resolution losses



H/A/α Decomposition

Asymptotic MLE approach

Results in a non-invertible equations system

$$\lambda_i = l_i + \frac{l_i}{n} \sum_{j \neq i}^m \frac{l_j}{l_i - l_j} + O(n^{-1}) \quad i = 1, 2, \dots, m$$

Sample eigenvalues are asymptotic estimators of the true eigenvalues



Speckle noise introduces an asymptotic bias on the sample eigenvalues

Asymptotic quasi MLE (AQ-MLE) approach

Necessity to simplify algebraic expressions in order to find an approximate solution for the equations system

AQ-MLE

$$\hat{\lambda}_i = \lambda_i - \frac{\lambda_i}{n} \sum_{j \neq i}^m \frac{\lambda_j}{\lambda_i - \lambda_j} - O(n^{-1}) \quad i = 1, 2, \dots, m.$$

Drawback: Error in the same order as the eigenvalues correction !!!

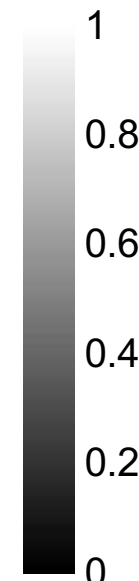
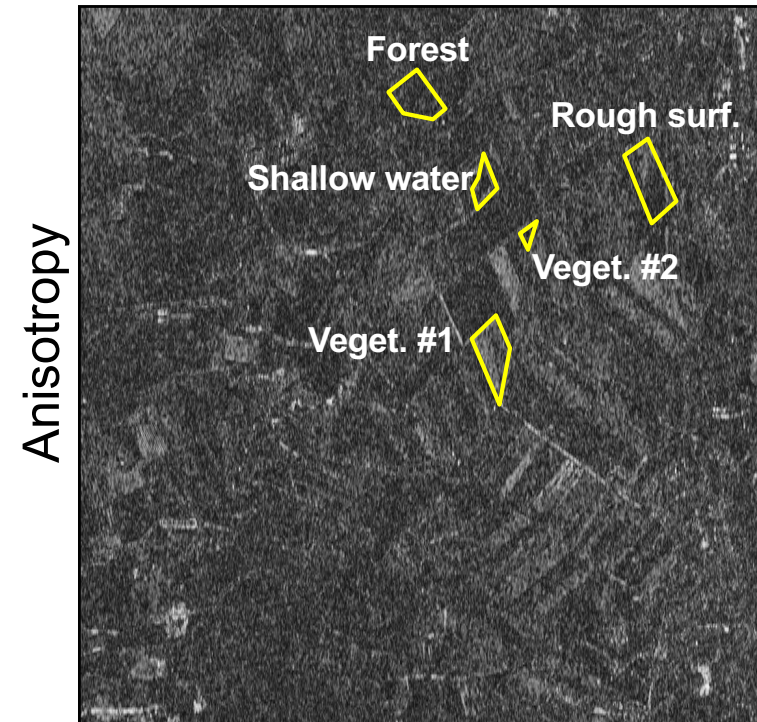
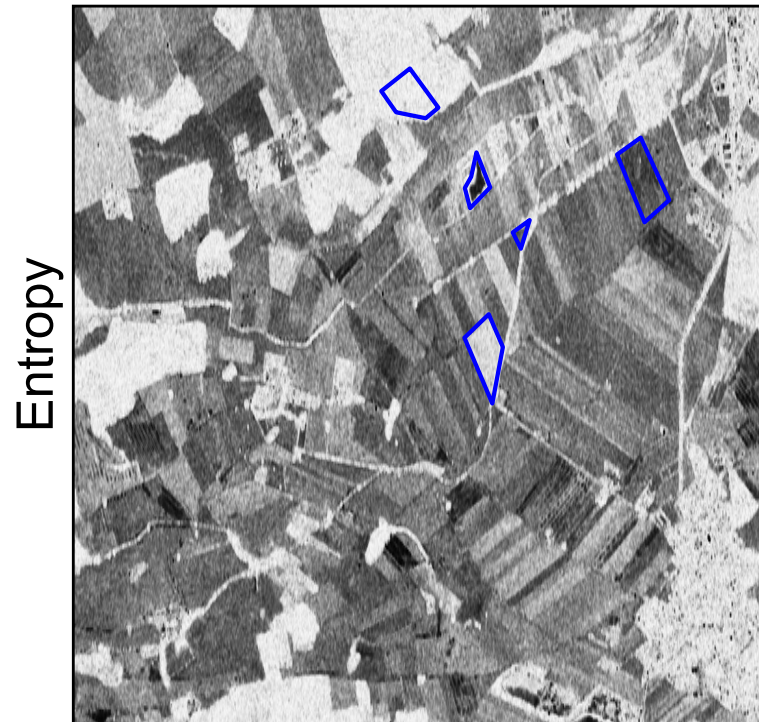
Fully polarimetric L-band dataset acquired with the E-SAR system



Data correspond to the ALLING test-site

Ground truth data available

5 homogeneous areas selected to cover all the Entropy (H) range

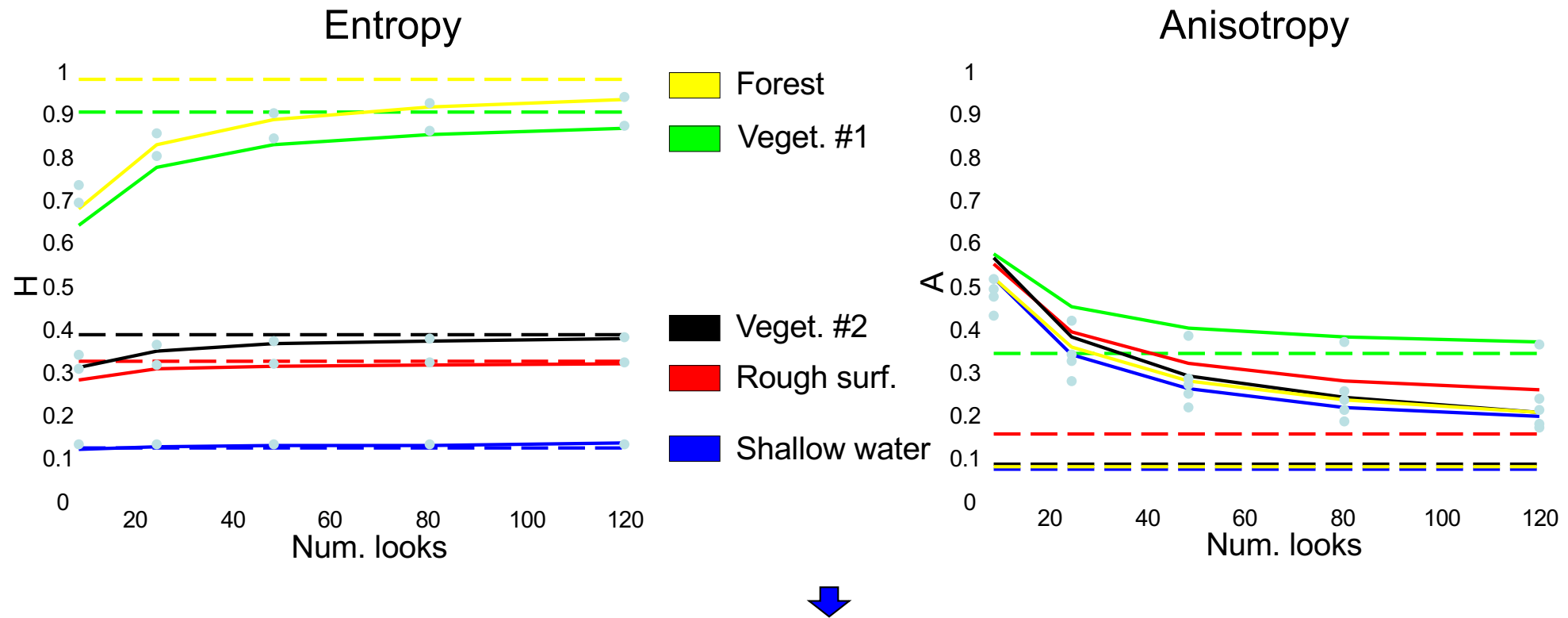


H/A/ α Decomposition

H/A estimated values

Dependence on the number of looks: $n \times n$ averaging windows

Dependence on the *true* values of H/A: Average over all the homogeneous area

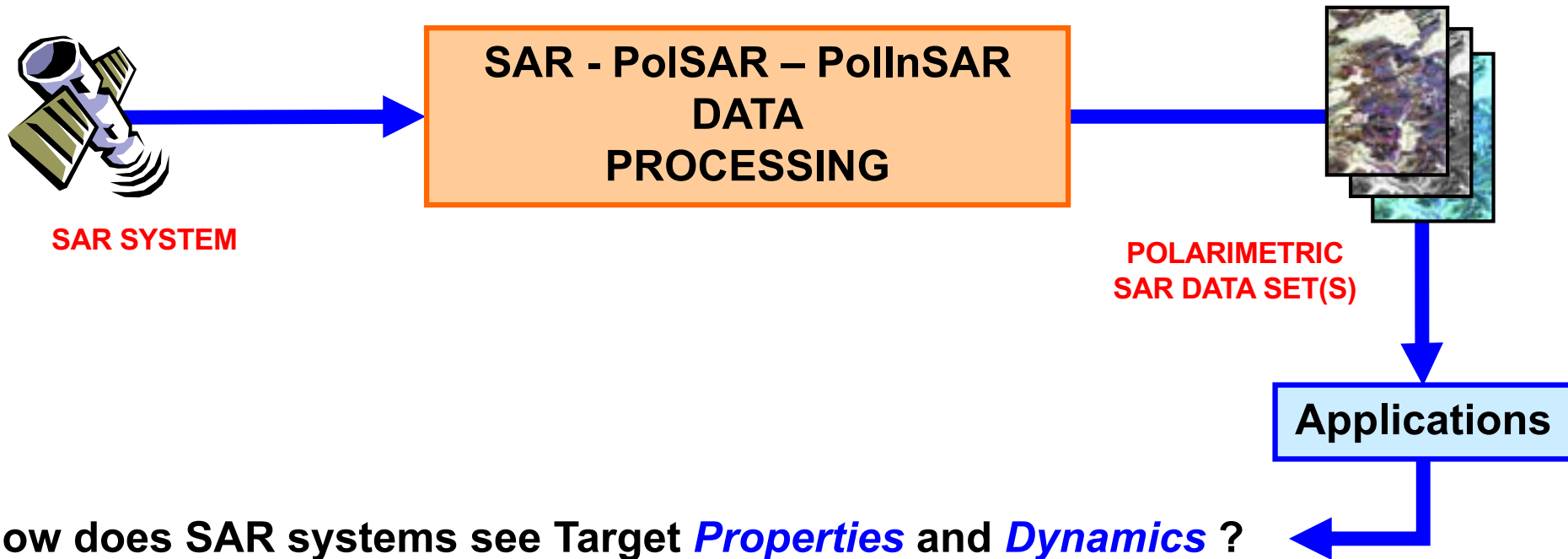


A minimum number of looks are necessary to retrieve unbiased physical parameters

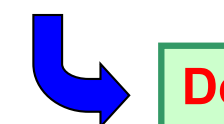


Forestry Applications

Introduction



How does SAR systems see Target *Properties* and *Dynamics* ?

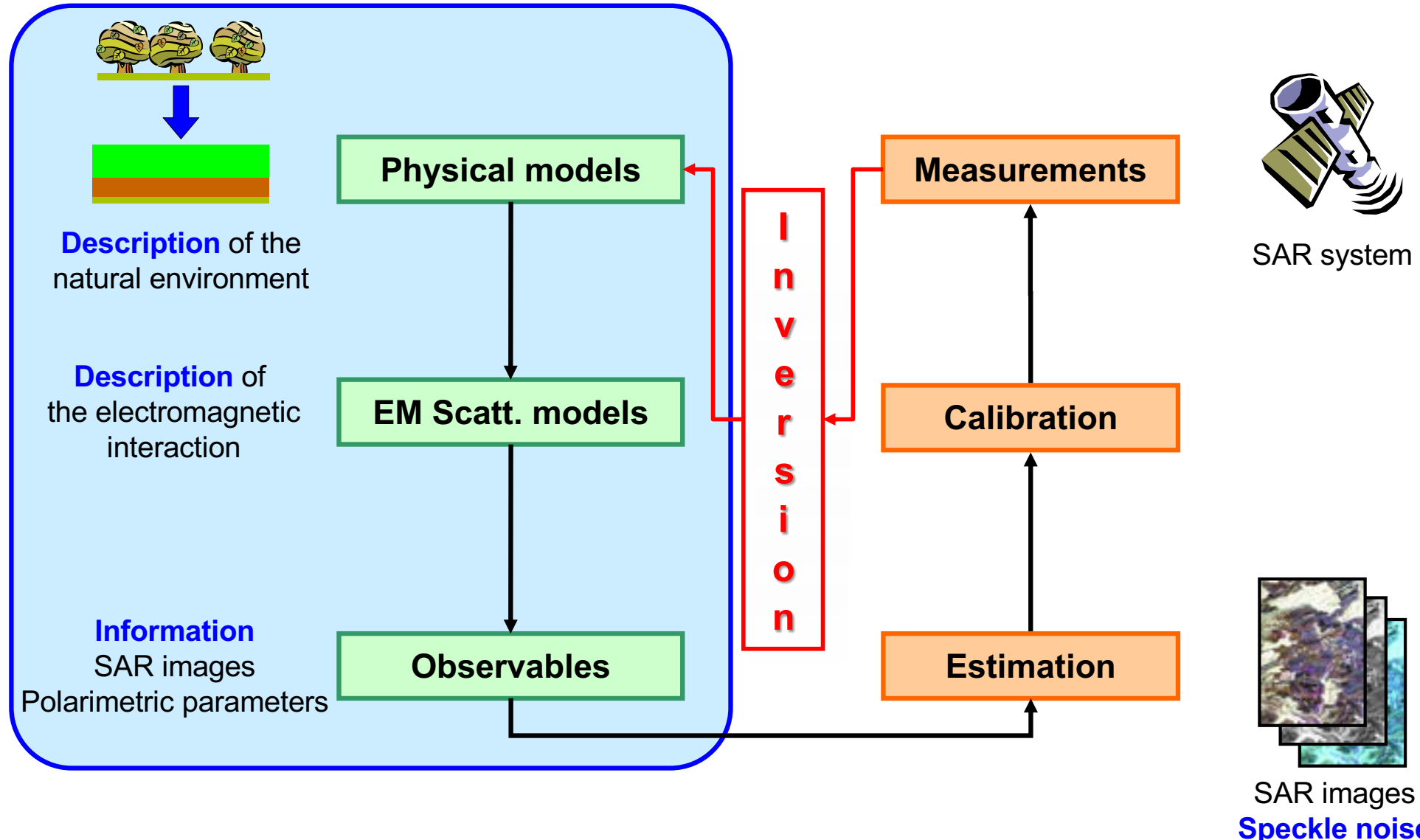


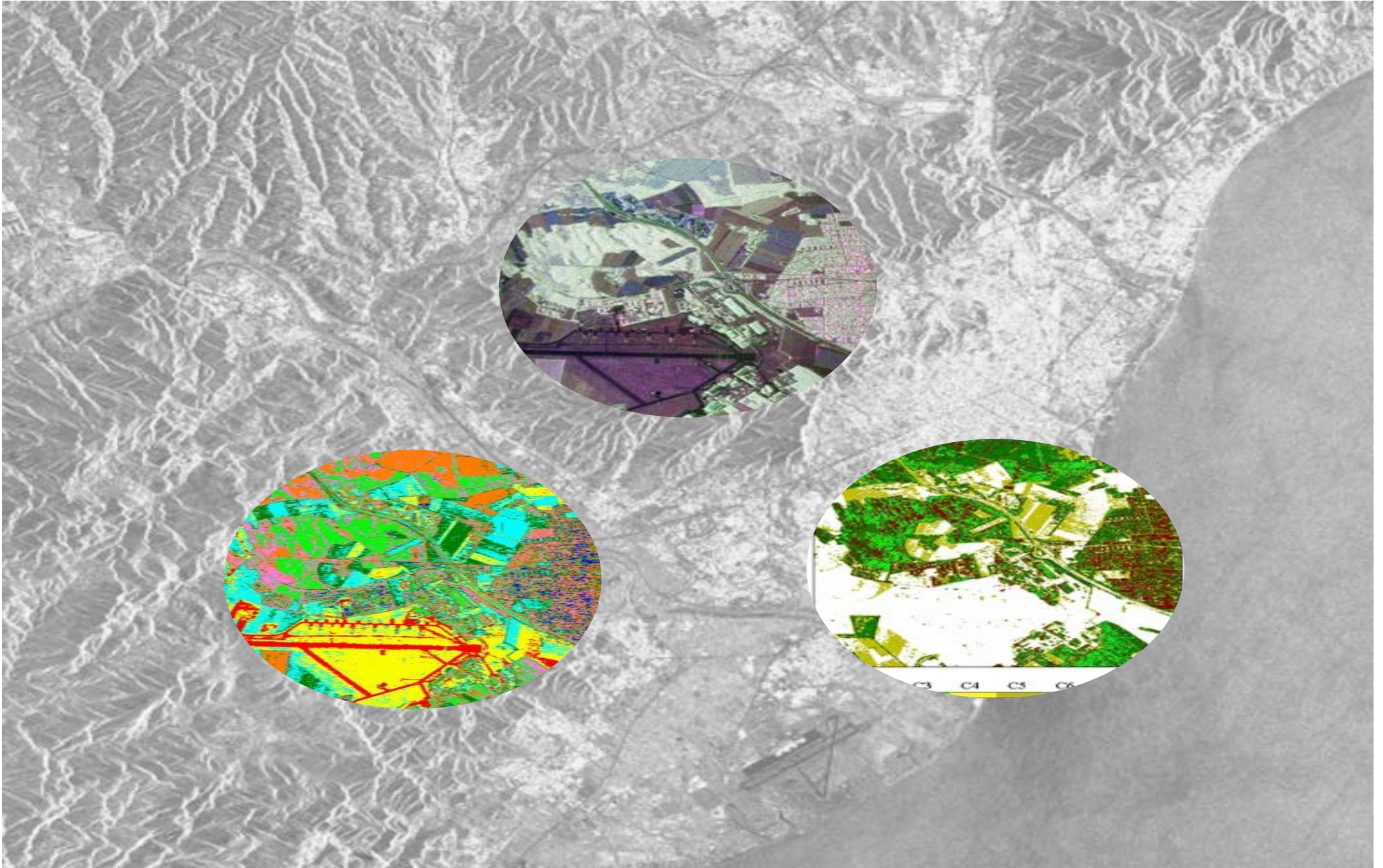
Define *FEASIBLE* applications



Determine signal processing tools, but *ADAPTED* to the data electromagnetic nature

Synthetic Aperture Imaging



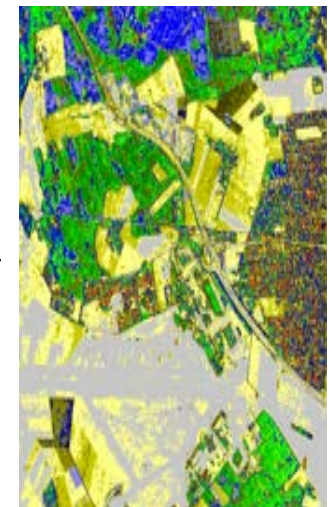
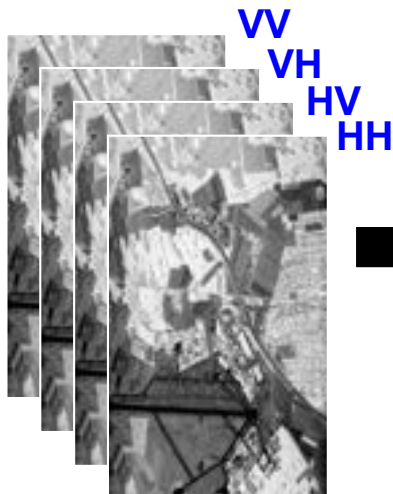


Thematic Classification

Supervised Classification

WISHART PDF

$$P(\langle \mathbf{T} \rangle / \mathbf{T}_m) = \frac{L^{Lp} |\langle \mathbf{T} \rangle|^{L-p} e^{-L \text{Tr}(\mathbf{T}_m^{-1} \langle \mathbf{T} \rangle)}}{\pi^{\frac{p(p-1)}{2}} \Gamma(L) \dots \Gamma(L-p+1) |\mathbf{T}_m|^L}$$



Wishart Classifier

Equivalent target vector distributions

- Lexicographic target vector

$$\underline{X} = [S_{HH} \quad \sqrt{2}S_{HV} \quad S_{VV}]^T$$

$$P(\underline{X}) = \frac{1}{\pi^3[C]} e^{-\underline{X}^{*T}[C]^{-1}\underline{X}}$$

- Pauli target vector

$$\underline{k} = \frac{1}{\sqrt{2}} [S_{HH} + S_{VV} \quad S_{HH} - S_{VV} \quad 2S_{HV}]^T \quad P(\underline{k}) = \frac{1}{\pi^3[T]} e^{-\underline{k}^{*T}[T]^{-1}\underline{k}}$$

The distributions are determined by the covariance or coherency matrices

$$\langle [T] \rangle = \frac{1}{N} \sum_{i=1}^N \underline{k}_i \cdot \underline{k}_i^{*T} = \frac{1}{N} \sum_{i=1}^N [T_i]$$

$$P(\langle [T] \rangle / [T_m]) = \frac{L^{Lp} |\langle [T] \rangle|^{L-p} e^{-LT_r([T_m]^{-1}\langle [T] \rangle)}}{\pi^{\frac{p(p-1)}{2}} \Gamma(L) \dots \Gamma(L-p+1) [T_m]^L}$$

COMPLEX WISHART DISTRIBUTION

L: Number of Look

p: Polarimetric Dimension

Wishart Classifier

$$P(\langle [T] \rangle / [T_m]) = \frac{L^{Lp} | \langle [T] \rangle |^{L-p} e^{-LTr([T_m]^{-1} \langle [T] \rangle)}}{\pi^{\frac{p(p-1)}{2}} \Gamma(L) \dots \Gamma(L-p+1) [T_m]^L}$$



SUPERVISED WISHART CLASSIFIER (Lee 1994)

BAYES MAXIMUM LIKELIHOOD CLASSIFICATION PROCEDURE

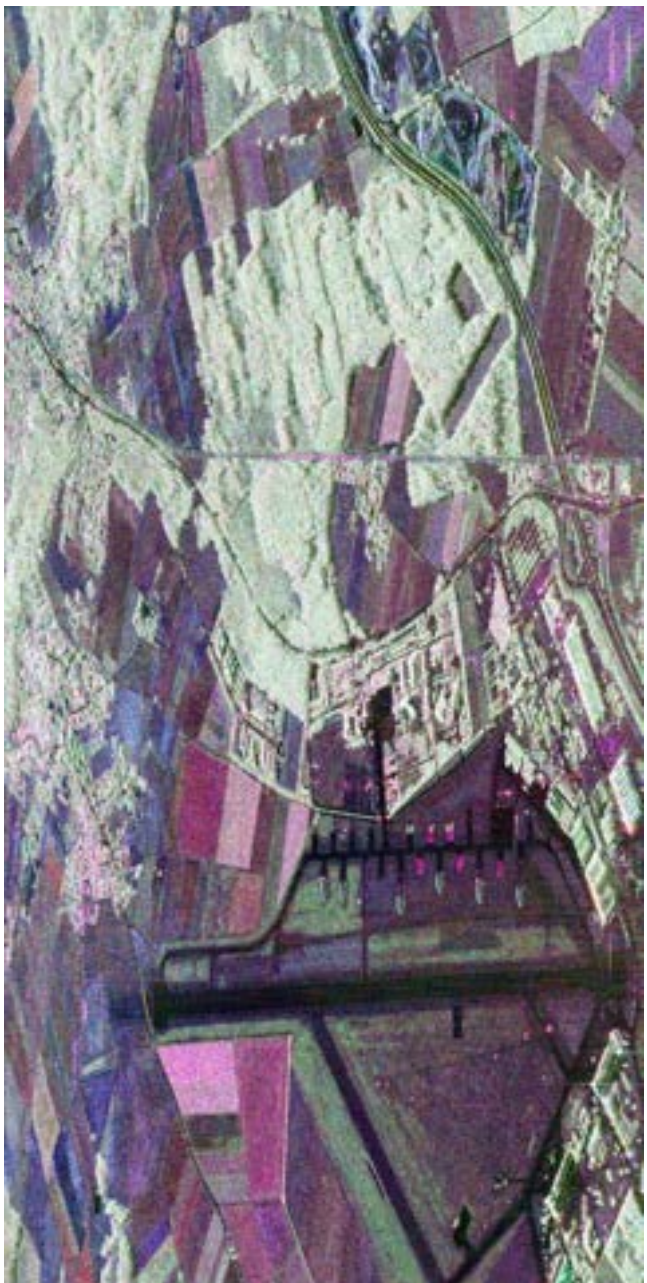
$$\langle [T] \rangle \in [T_m] \quad \text{if} \quad d_m(\langle [T] \rangle) < d_j(\langle [T] \rangle) \quad \forall j \neq m$$

with

$$d_m(\langle [T] \rangle) = LTr([T_m]^{-1} \langle [T] \rangle) + L \ln([T_m]) - \ln(P([T_m])) + K$$

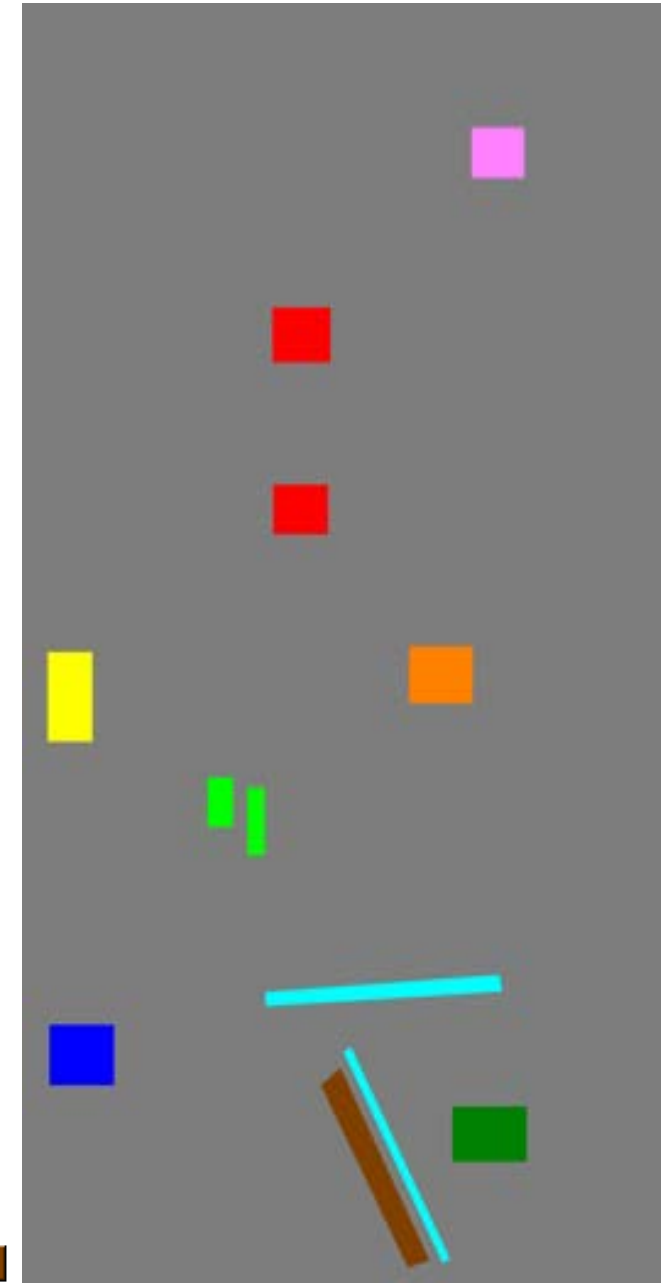
$[T_m]$: Cluster Center of the class m

Wishart Classifier



|Shh-Svv| 2|Shv| | Shh +Svv|

Training areas



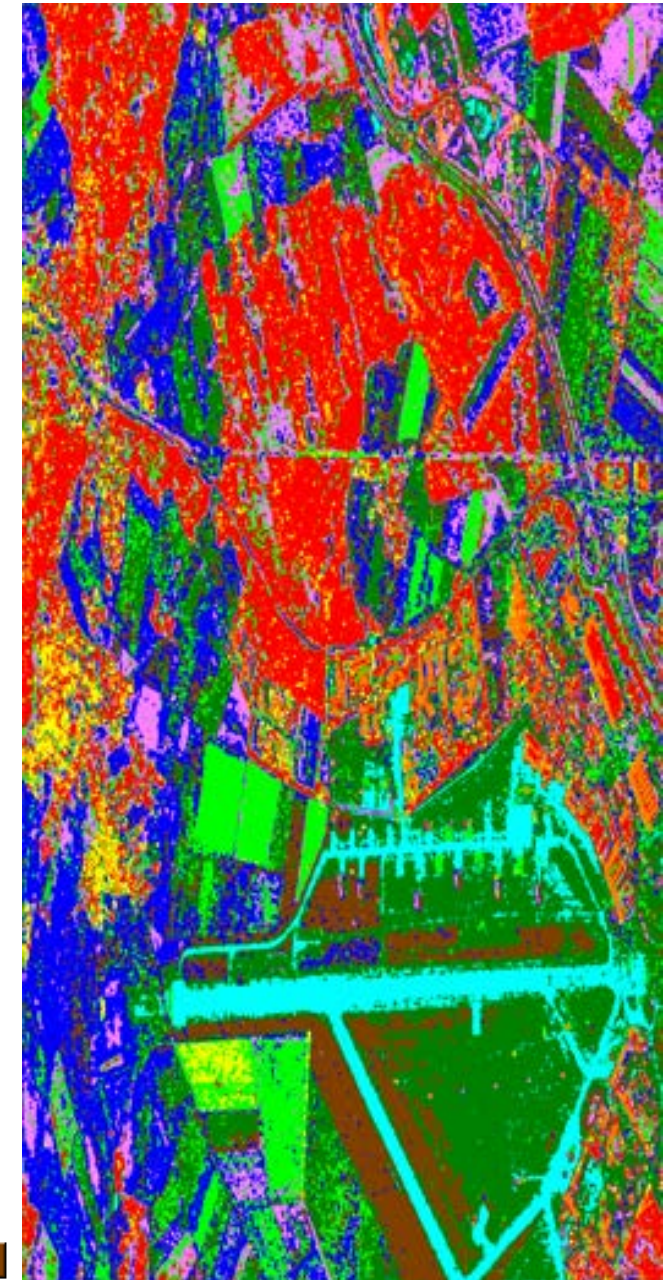
Wishart Classifier



|Shh-Svv| 2|Shv| | Shh +Svv|

Classification
results

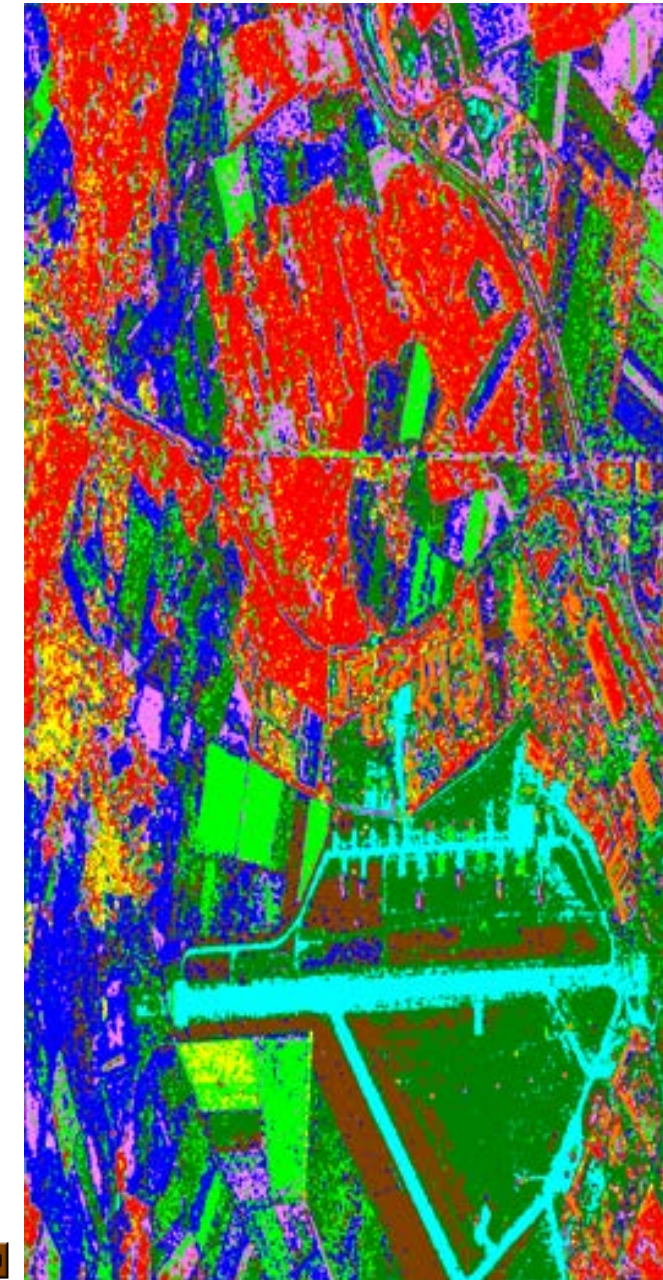
01 02 03 04 05 06 07 08 09



Wishart Classifier

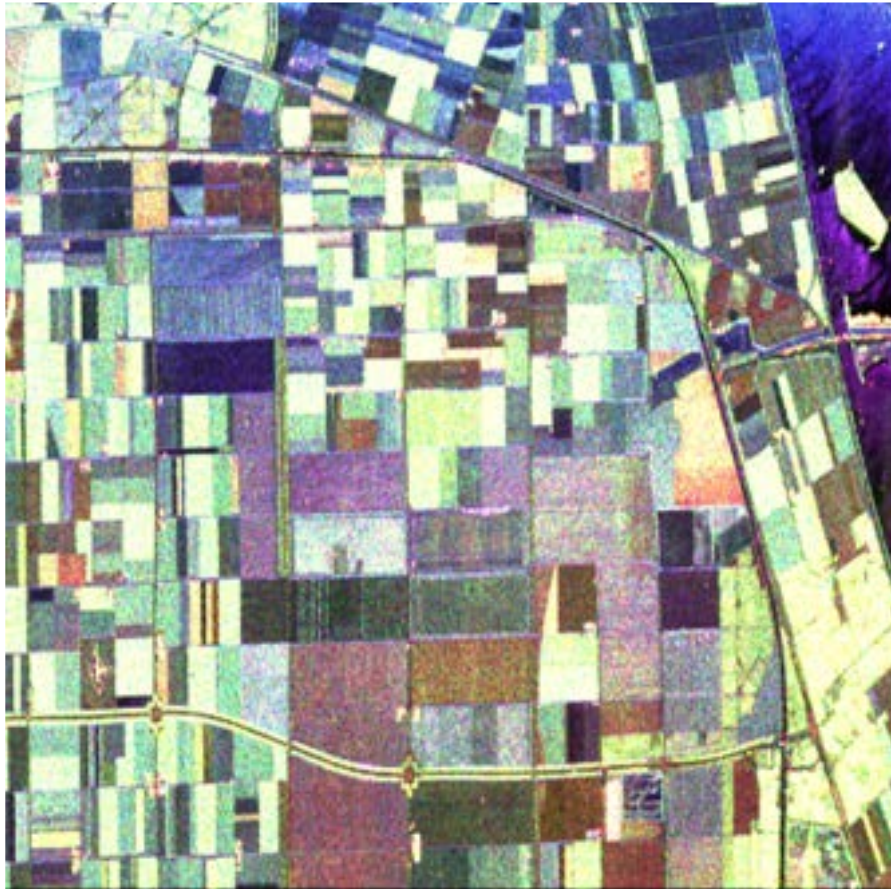
Confusion matrix

	C1	C2	C3	C4	C5	C6	C7	C8	C9
C1	90.43	2.58	0.06	5.20	1.35	0.00	0.00	0.31	0.07
C2	0.09	99.60	0.00	0.00	0.00	0.00	0.00	0.31	0.00
C3	0.90	7.60	66.02	0.02	0.00	1.37	0.00	11.23	12.85
C4	28.53	11.67	5.29	36.96	7.97	0.48	0.00	7.77	1.33
C5	20.97	19.26	7.67	3.57	26.48	5.69	0.19	9.62	6.55
C6	0.00	0.14	0.00	0.00	0.00	98.83	0.96	0.00	0.07
C7	0.00	0.00	0.00	0.00	0.00	0.03	99.97	0.00	0.00
C8	5.92	5.64	11.56	3.99	0.52	20.06	6.03	35.24	11.03
C9	0.00	0.00	2.17	0.00	0.00	0.31	0.00	0.09	97.43



Wishart Classifier

Courtesy of Dr J.S Lee



$|HH+VV|$

$|HV|$

$|HH-VV|$

JPL AIRSAR
P-L-C Band Flevoland Data



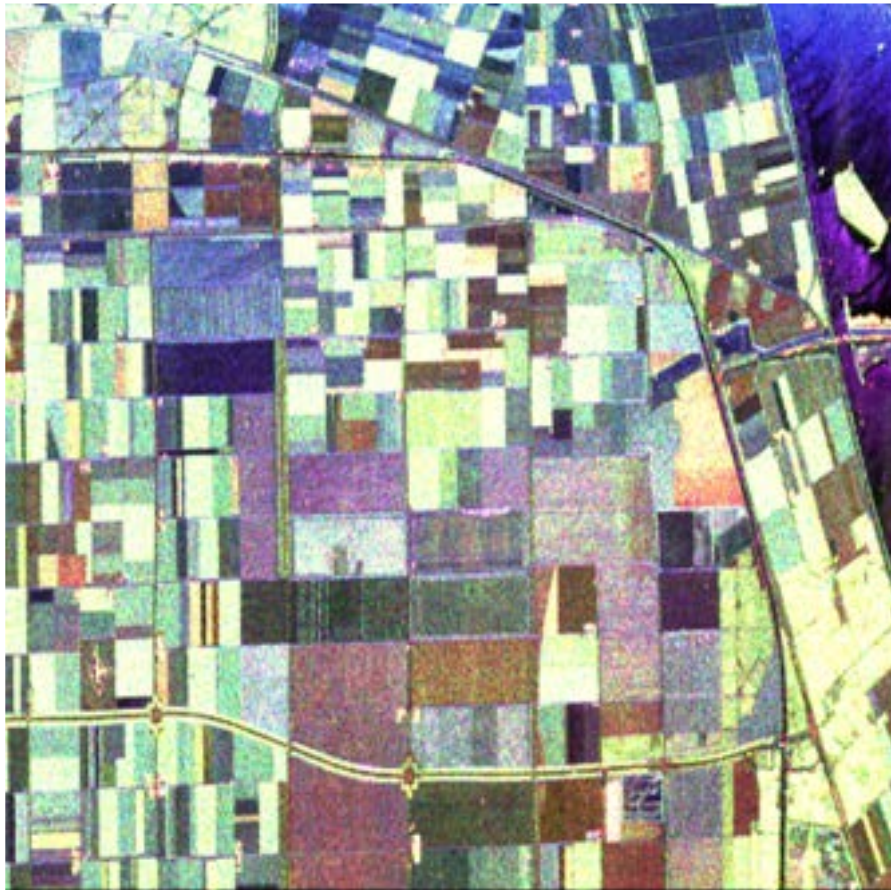
Stembeans Lucerne Rapeseed
 Forest Wheat Peas
 Water Baresoil Grass
 Potatoes Beet

Original Ground- Truth



Wishart Classifier

Courtesy of Dr J.S Lee



|HH+VV|

|HV|

|HH-VV|

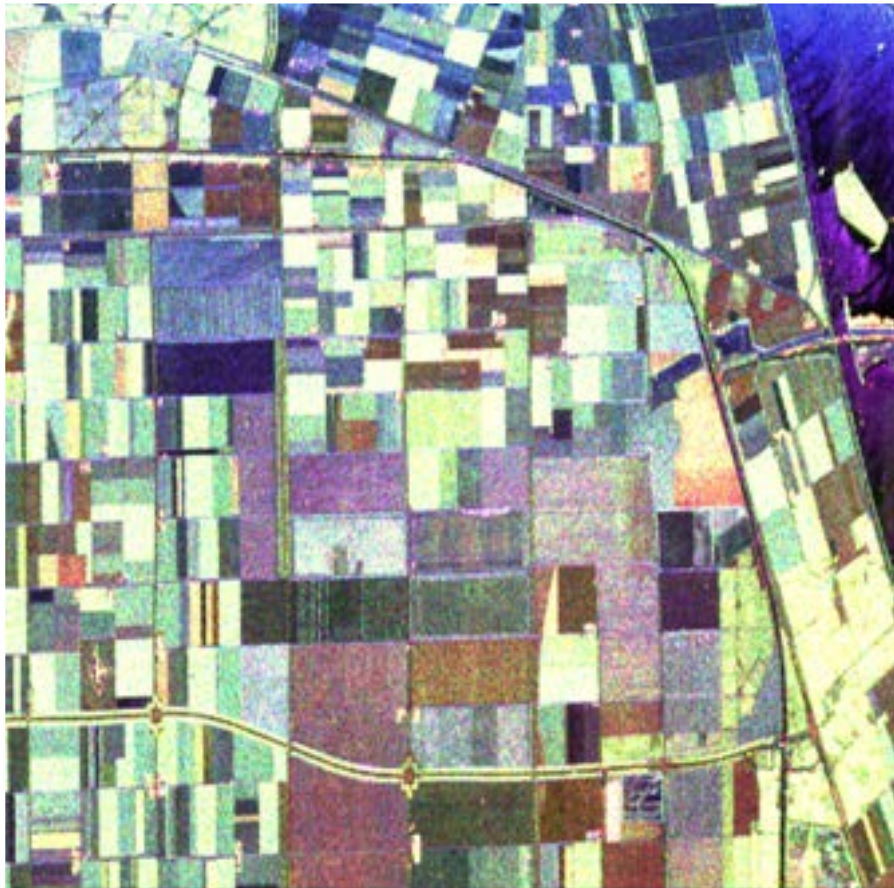
JPL AIRSAR
L-Band Flevoland Data



C-band (66.53%)

Wishart Classifier

Courtesy of Dr J.S Lee



|HH+VV|

|HV|

|HH-VV|

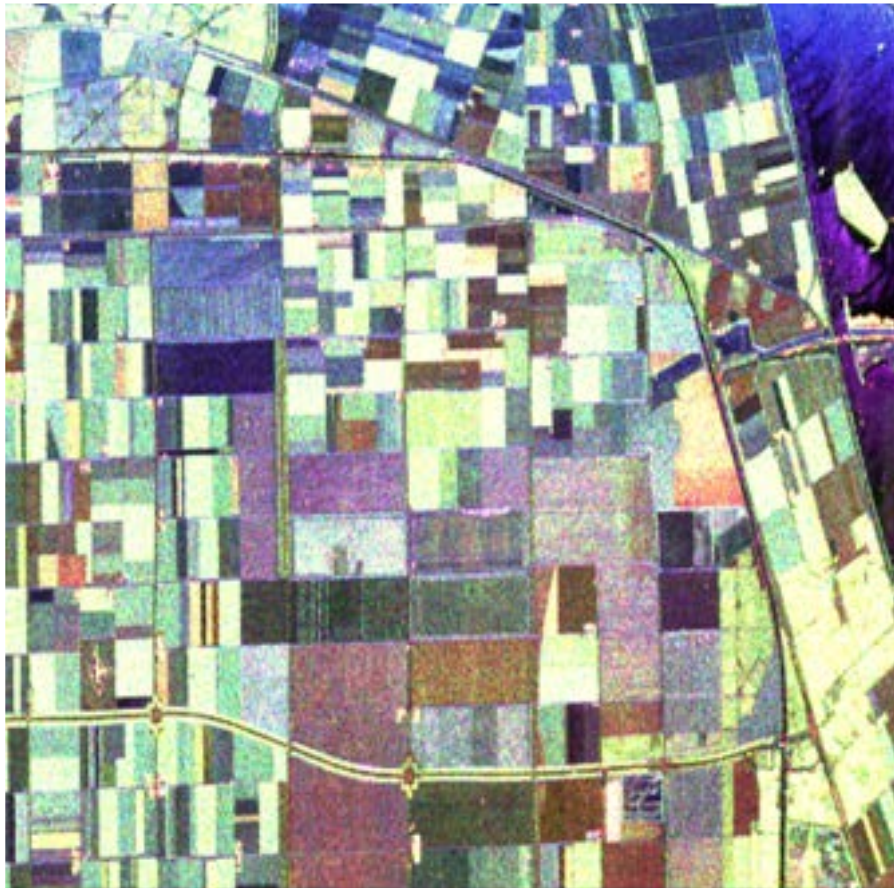
JPL AIRSAR
L-Band Flevoland Data



L-band (81.63%)

Wishart Classifier

Courtesy of Dr J.S Lee

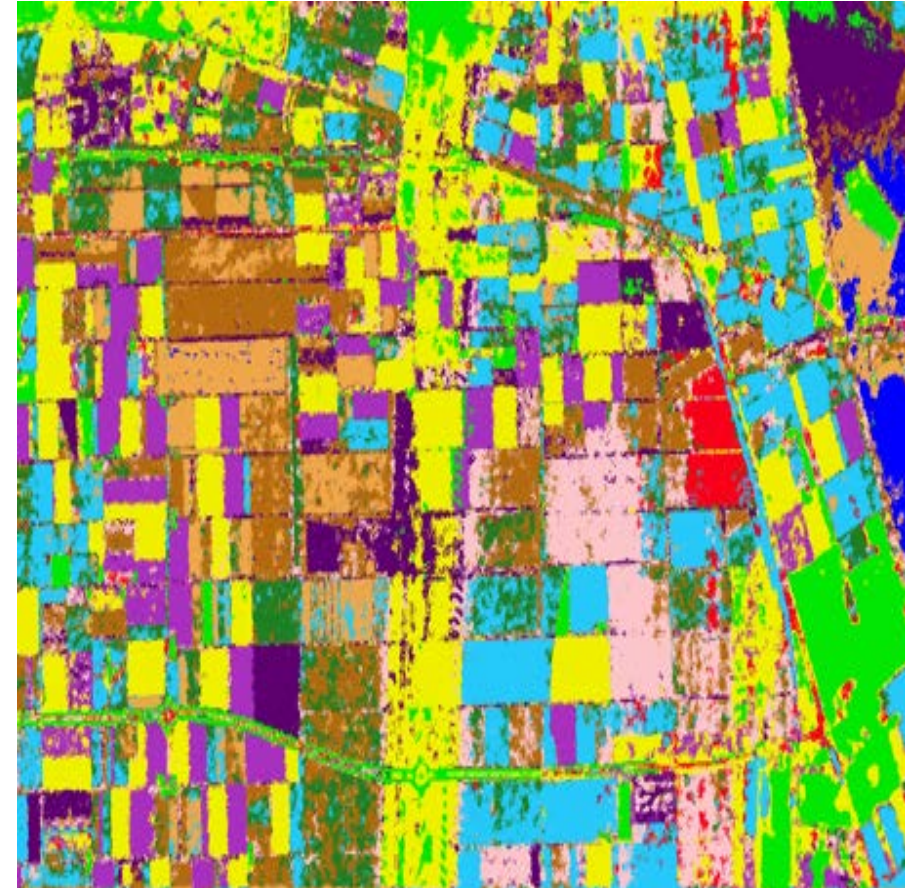


|HH+VV|

|HV|

|HH-VV|

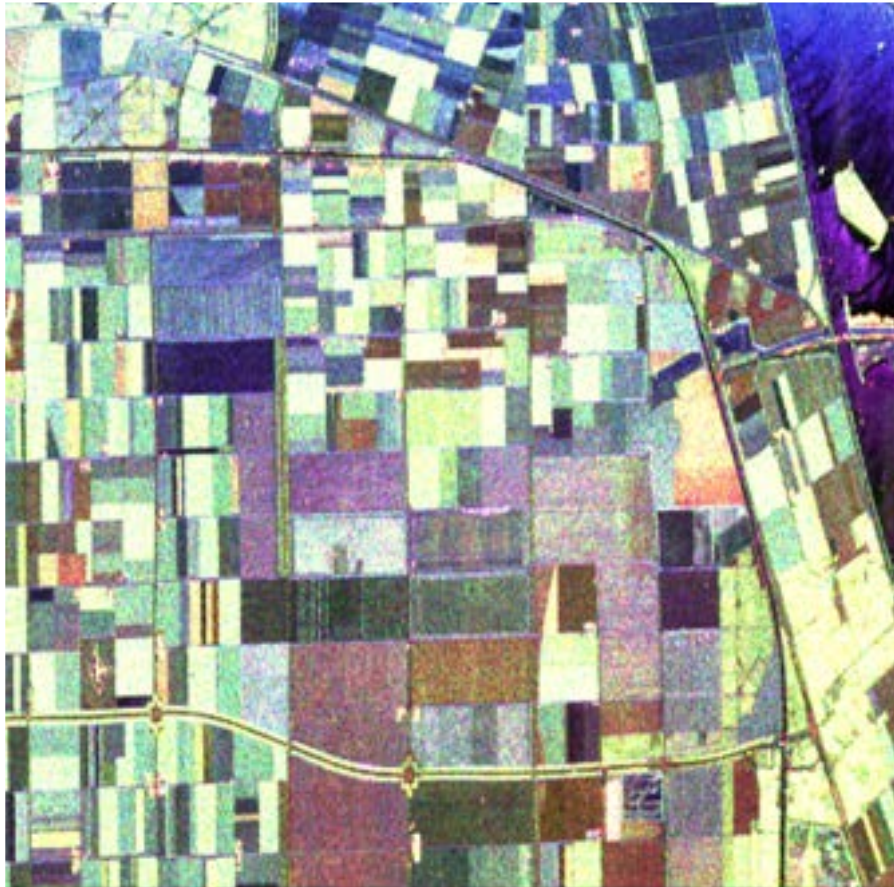
JPL AIRSAR
L-Band Flevoland Data



P-band (71.37%)

Wishart Classifier

Courtesy of Dr J.S Lee

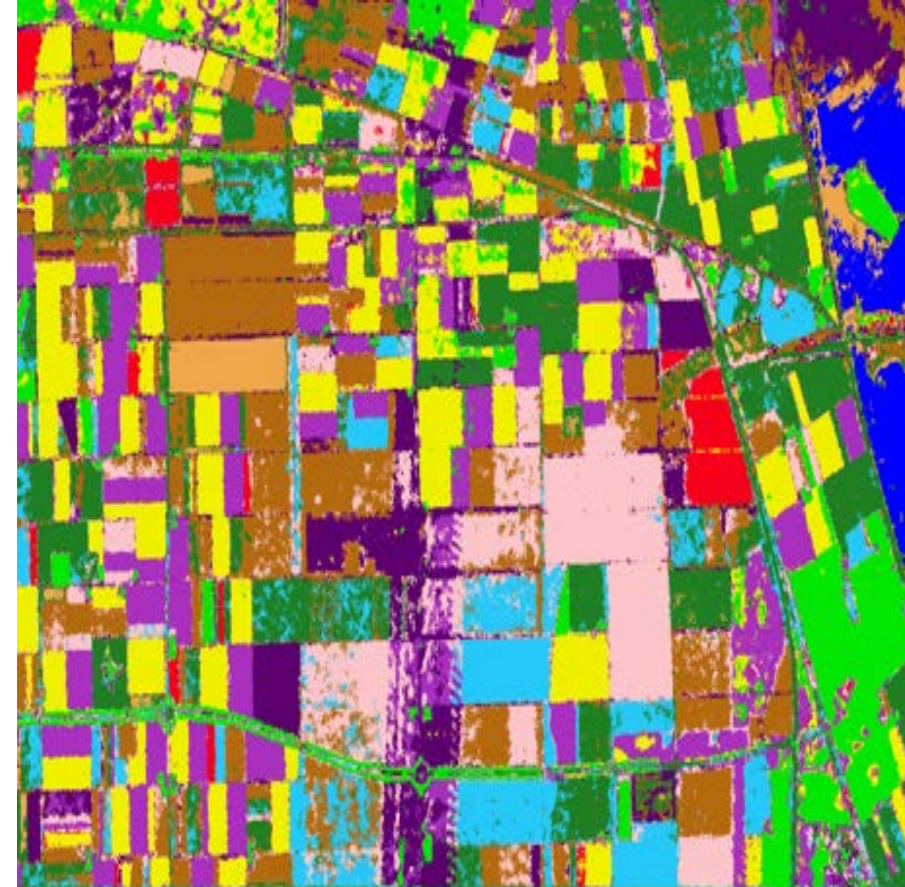


|HH+VV|

|HV|

|HH-VV|

JPL AIRSAR
L-Band Flevoland Data



P-L-C band (91.21%)

Supervised Classifier

For crop classification

- L-band is better than P-Band and C-band
- Dual-polarization HH and VV with coherence (Including phase differences) is almost as good as fully polarimetric

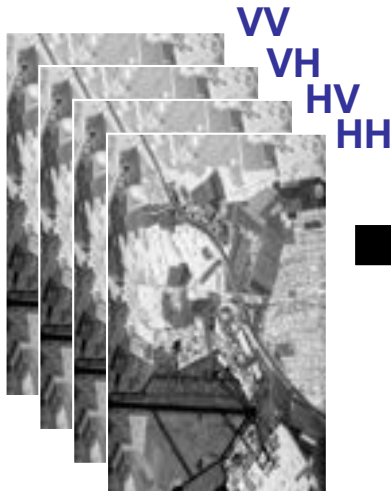
For forest classification

- P-band is better than L- and C-band
- HV is the most important polarization
- Coherence is not important for classification

Unsupervised Classification

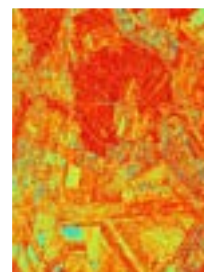
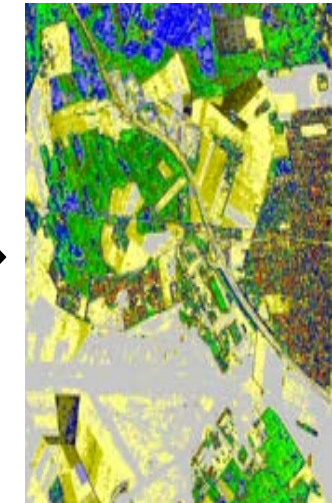
WISHART PDF

$$P(\langle [T] \rangle / [T_m]) = \frac{L^{Lp} | \langle [T] \rangle |^{L-p} e^{-LT_r([T_m]^{-1} \langle [T] \rangle)}}{\pi^{\frac{p(p-1)}{2}} \Gamma(L) \dots \Gamma(L-p+1) [T_m]^L}$$

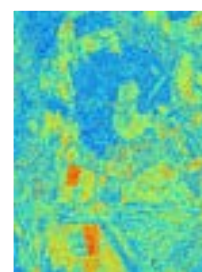


UNSUPERVISED POLSTAR CLASSIFICATION

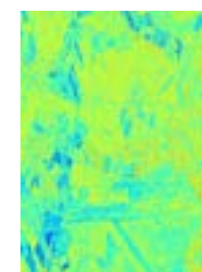
E.POTTIER, J.S LEE (2000)



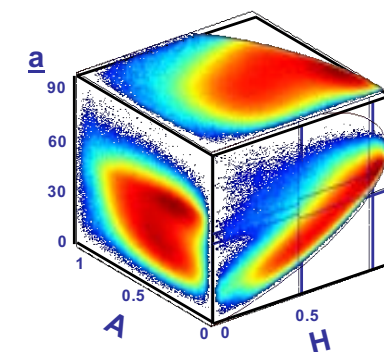
H



A

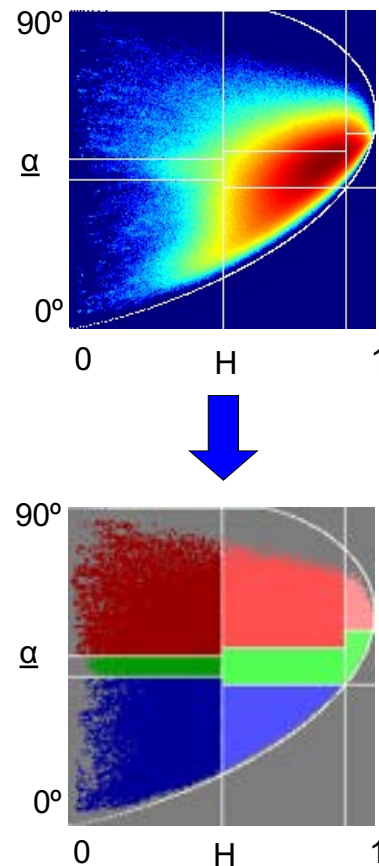
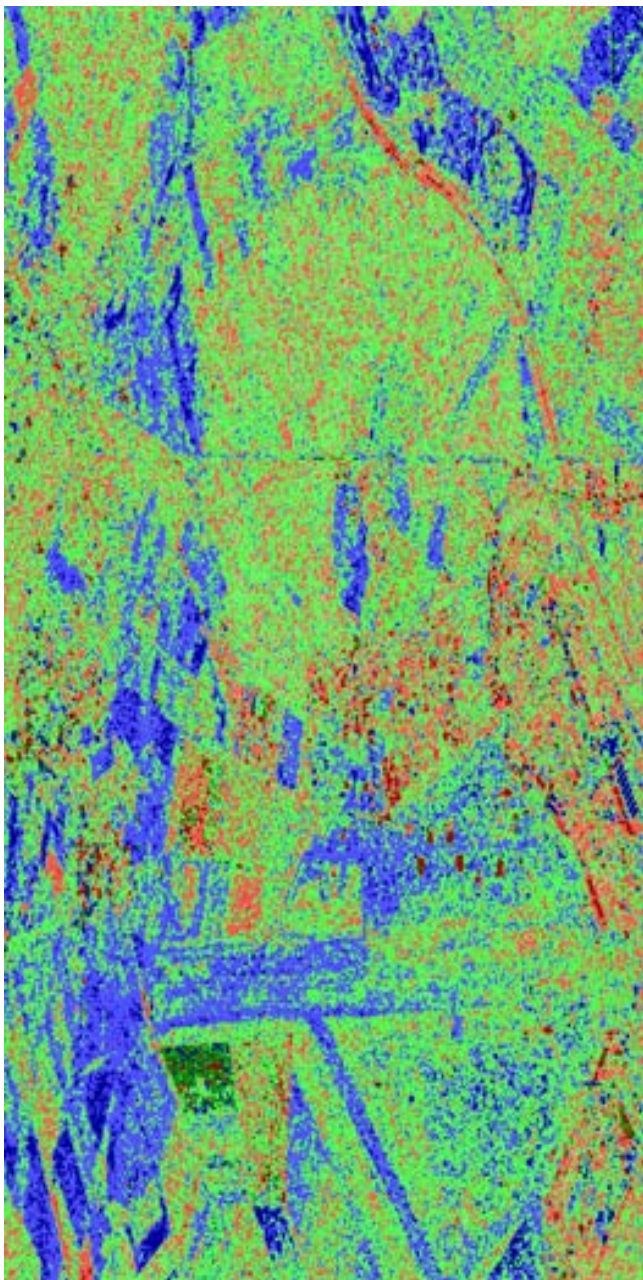


α



H / A / α DECOMPOSITION THEOREM

H/ α Classification



H / α classification space
Sub-divided into 9 basic zones
(Basic scattering mechanisms)



Arbitrary boundaries

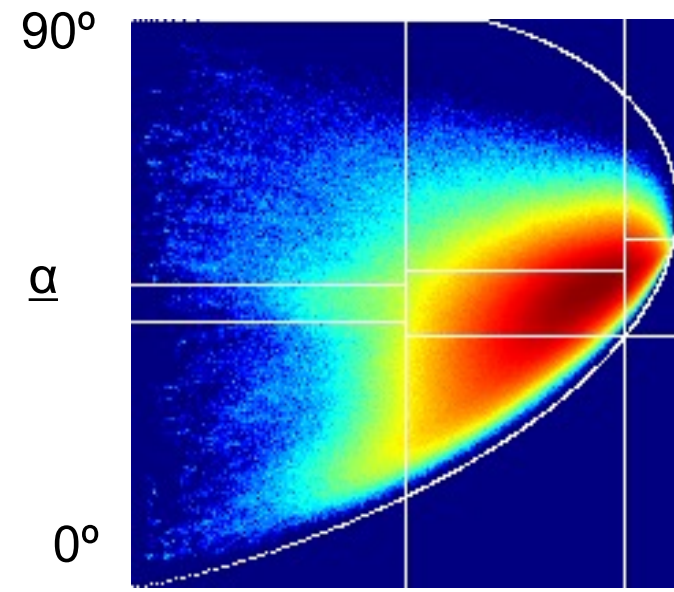
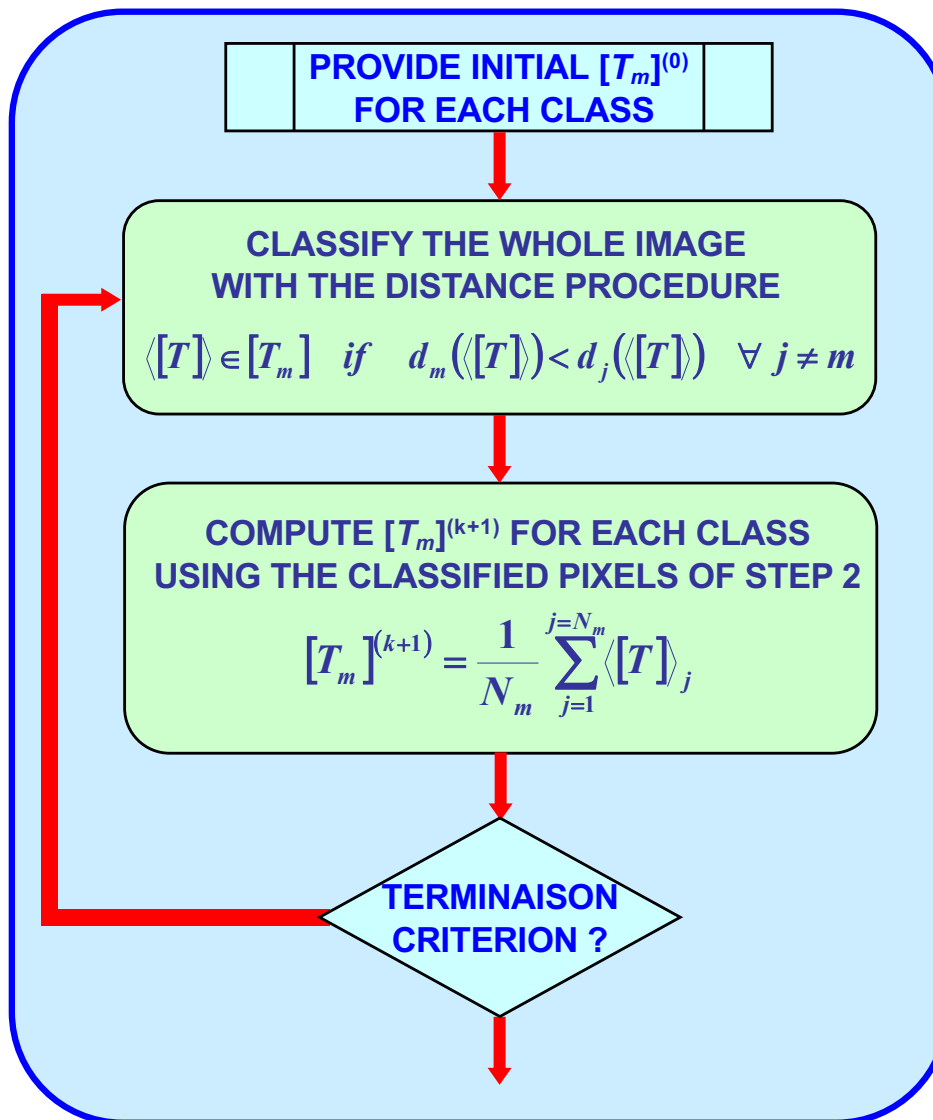
Degree of arbitrariness on the setting of these boundaries



Segmentation is offered merely to illustrate the unsupervised classification strategy and to emphasize the geometrical segmentation of physical scattering processes

H/ α Wishart Classifier

K-mean classification procedure

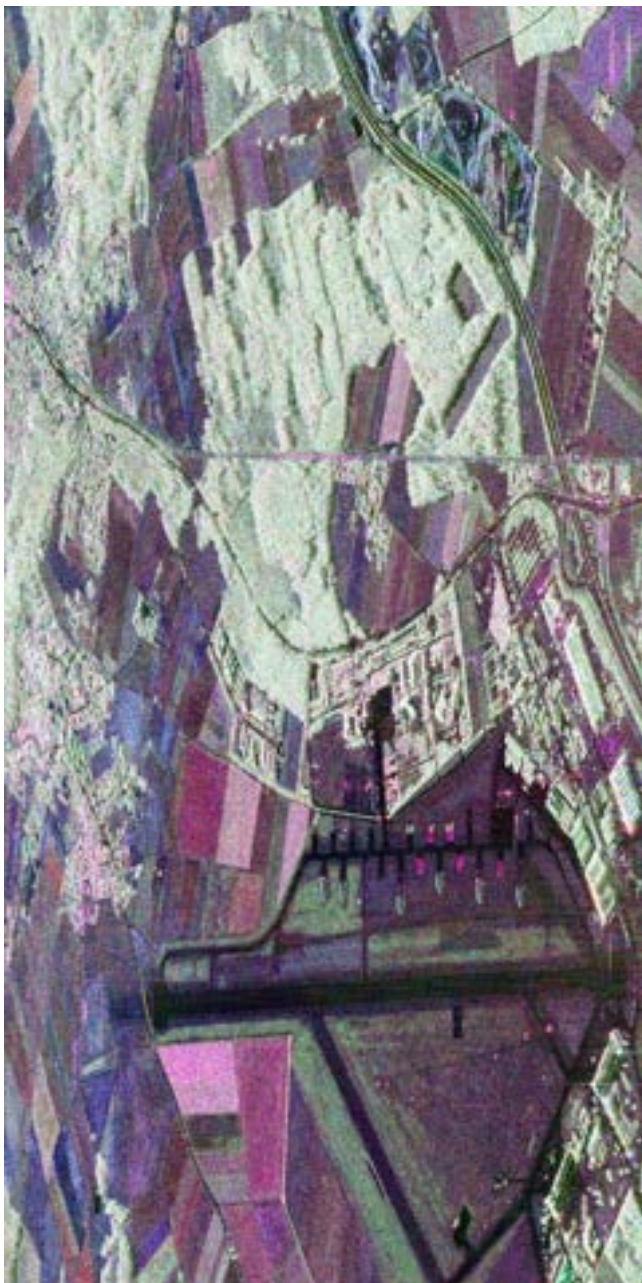


$$H$$

$$[T_m]^{(0)} = \frac{1}{N_m} \sum_{k=1}^{k=N_m} \langle [T] \rangle_k$$

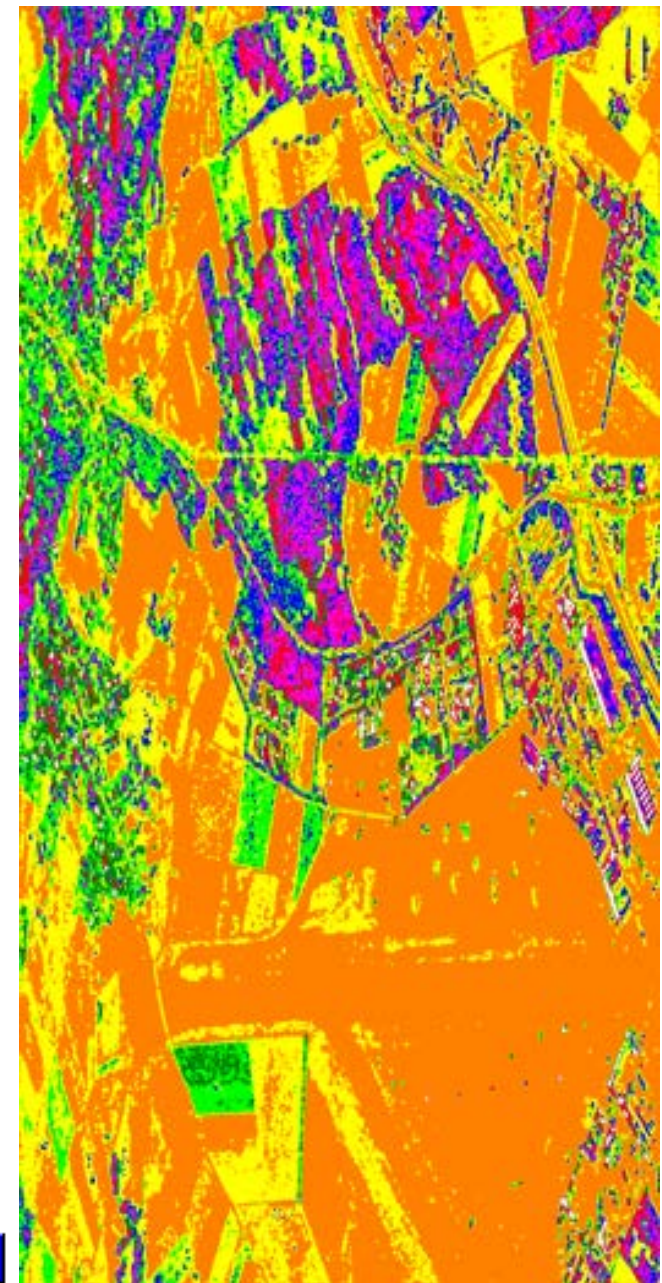
Cluster Center of the class m
(Lee 1998)

H/ α Wishart Classifier

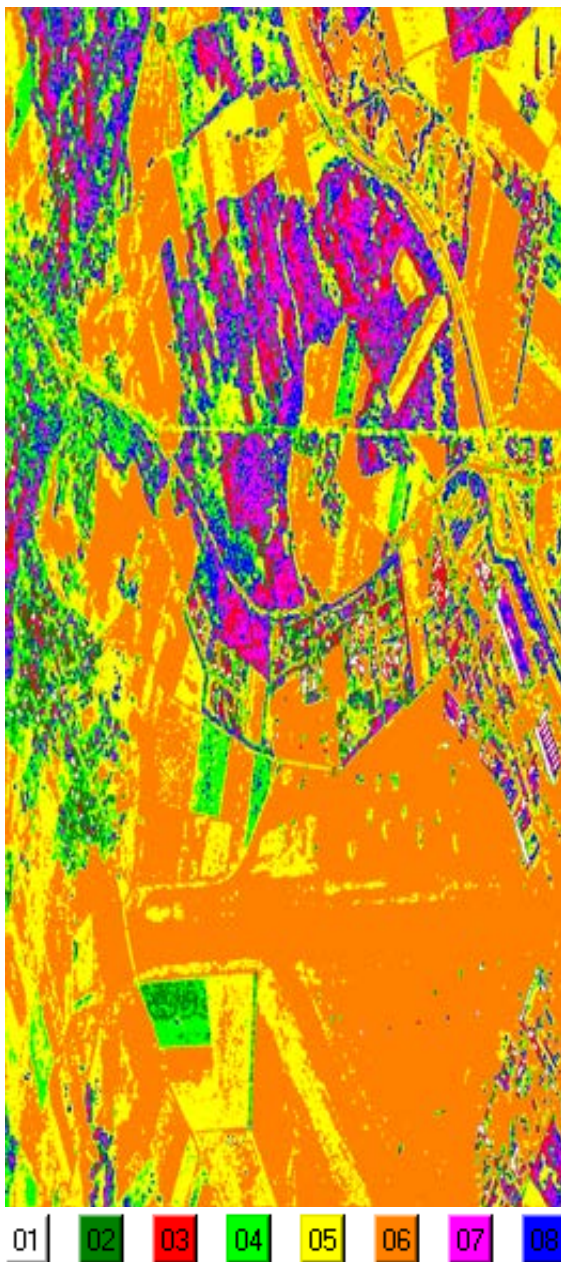


|Shh-Svv| 2|Shv| | Shh +Svv|

01 02 03 04 05 06 07 08



H/ α Wishart Classifier



During classification, the cluster centers may move out their zones or several clusters may end in the same zone



Identification of the terrain type may cause some confusion due to the color scheme



The combined Wishart classifier is extended and complemented with the introduction of the Anisotropy (A)



More classes available
more sensitivity to classify areas with high Entropy

H/ α Wishart Classifier

SAN FRANCISCO BAY JPL - AIRSAR L-band 1988



|HH+VV|

|HV|

|HH-VV|

C1 C2 C3 C4 C5 C6 C7 C8



SpaceSUITE

45

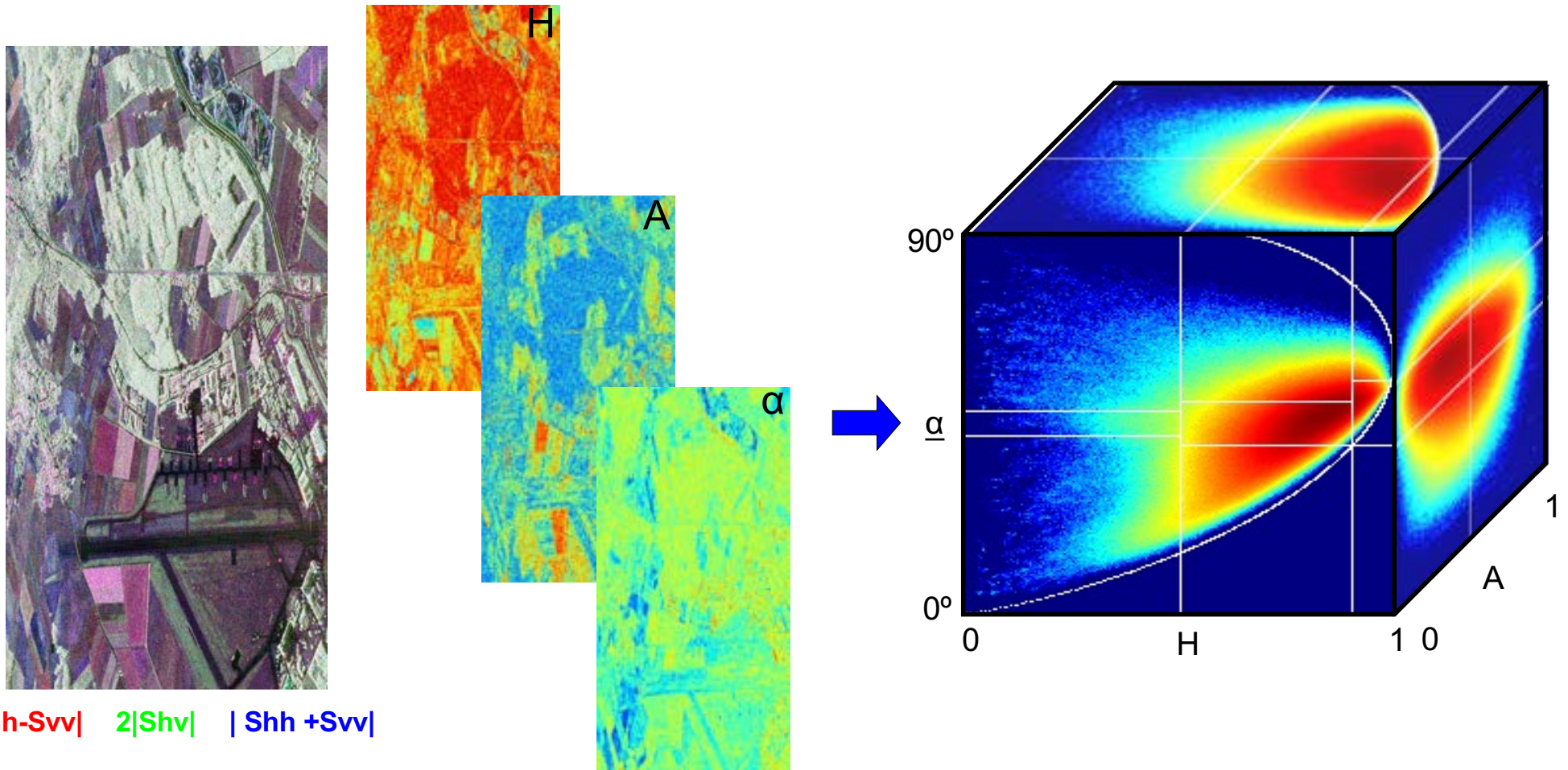


UNIVERSITAT POLITÈCNICA DE CATALUNYA
BARCELONATECH
Department of Signal Theory
and Communications

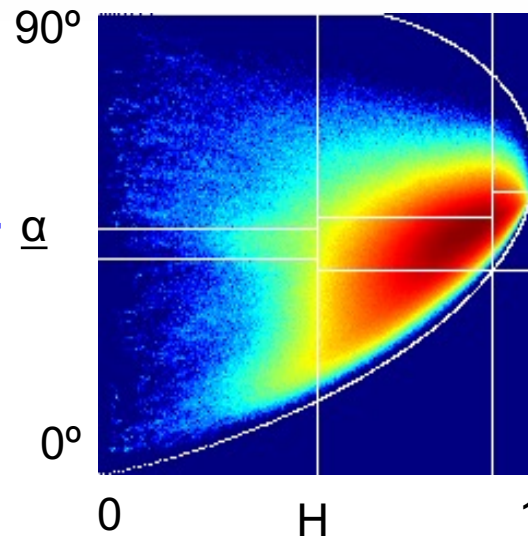
IEEC

H/A/ α Wishart Classifier

PolSAR data distribution in the H/A/ α plane

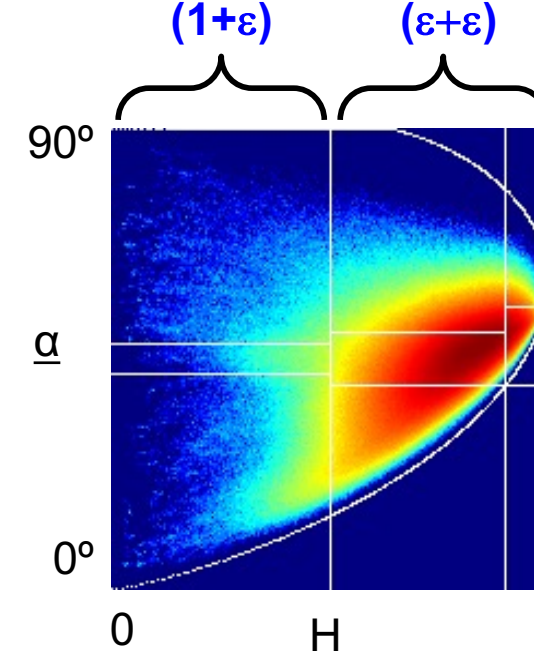
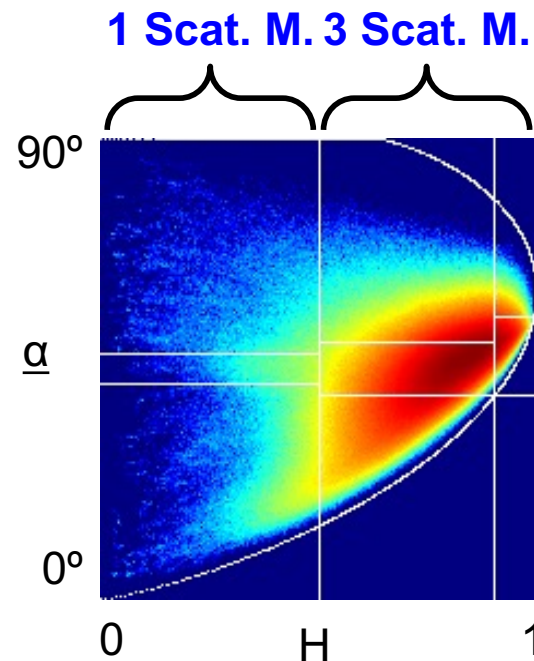


H/A/ α Wishart Classifier



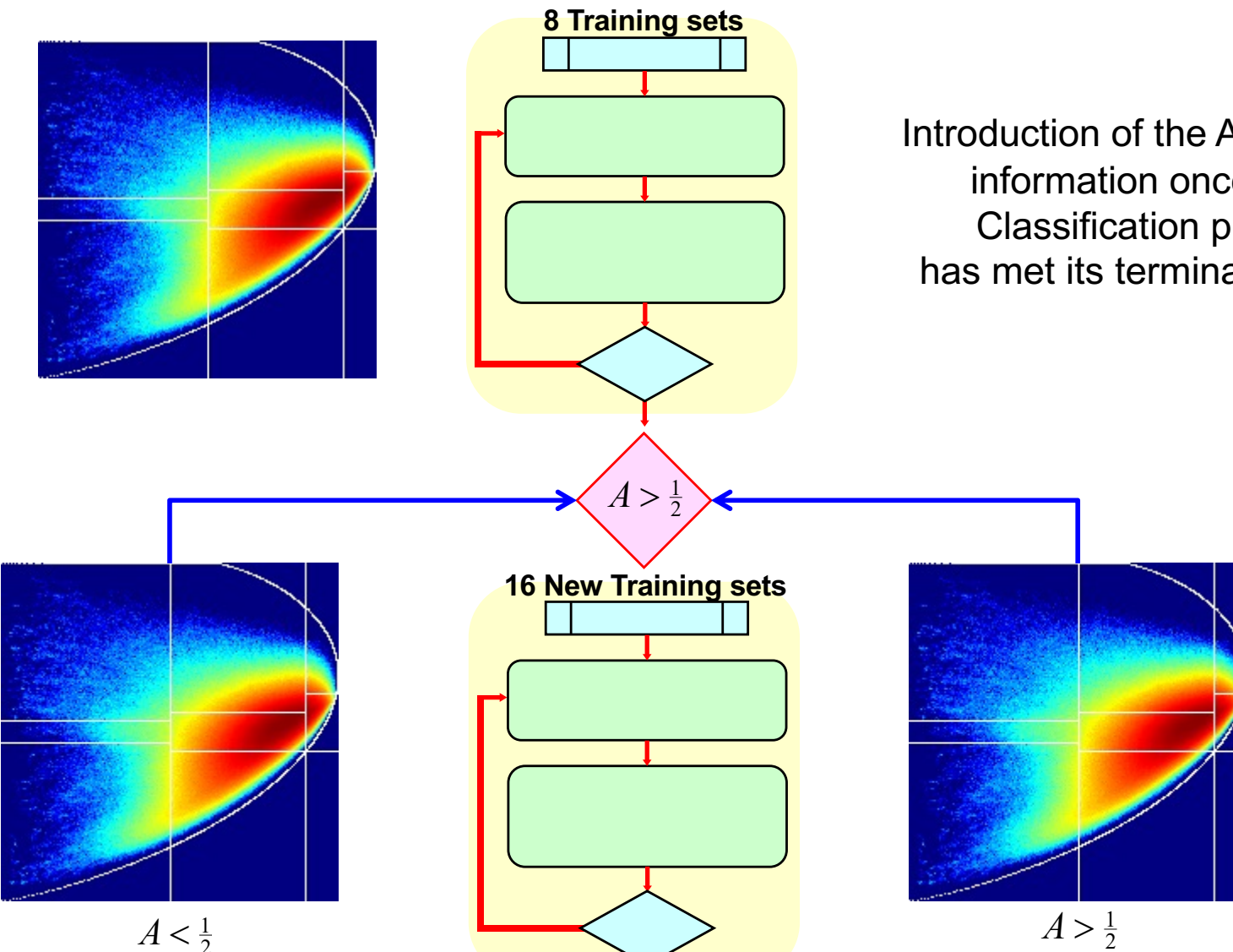
$A > 0.5$
 $\lambda_2 \gg \lambda_3$

3 Scat. M.



H/A/ α Wishart Classifier

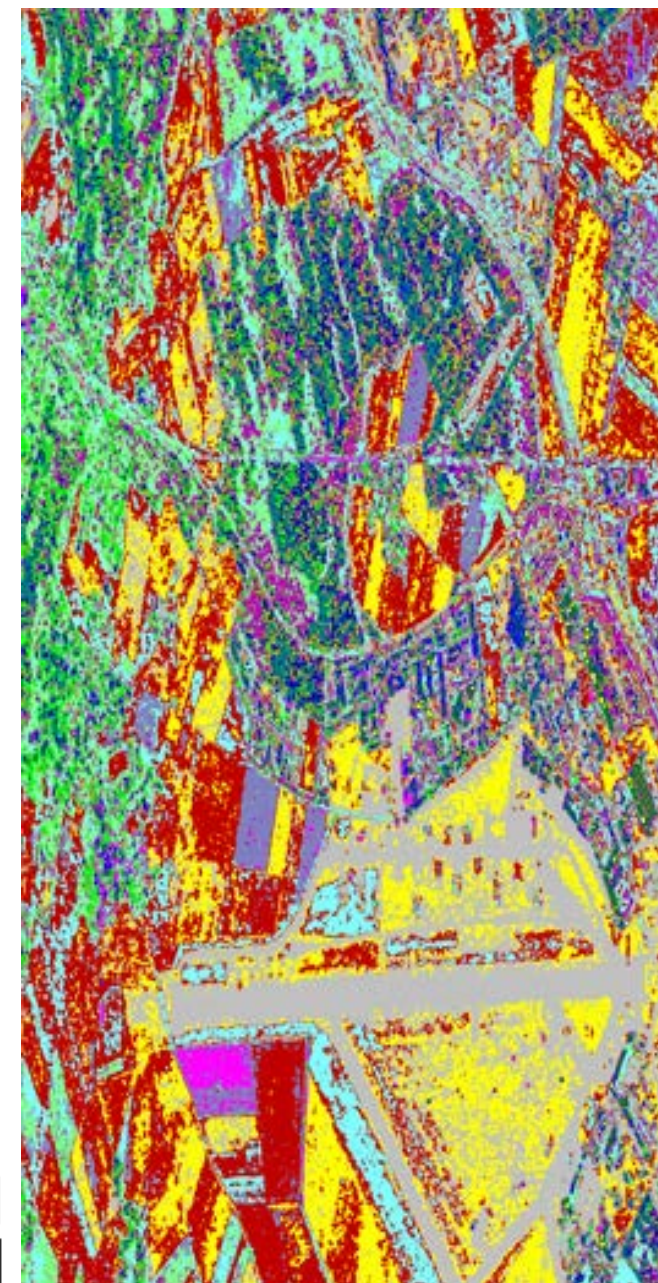
2 successive k - mean Classification procedures



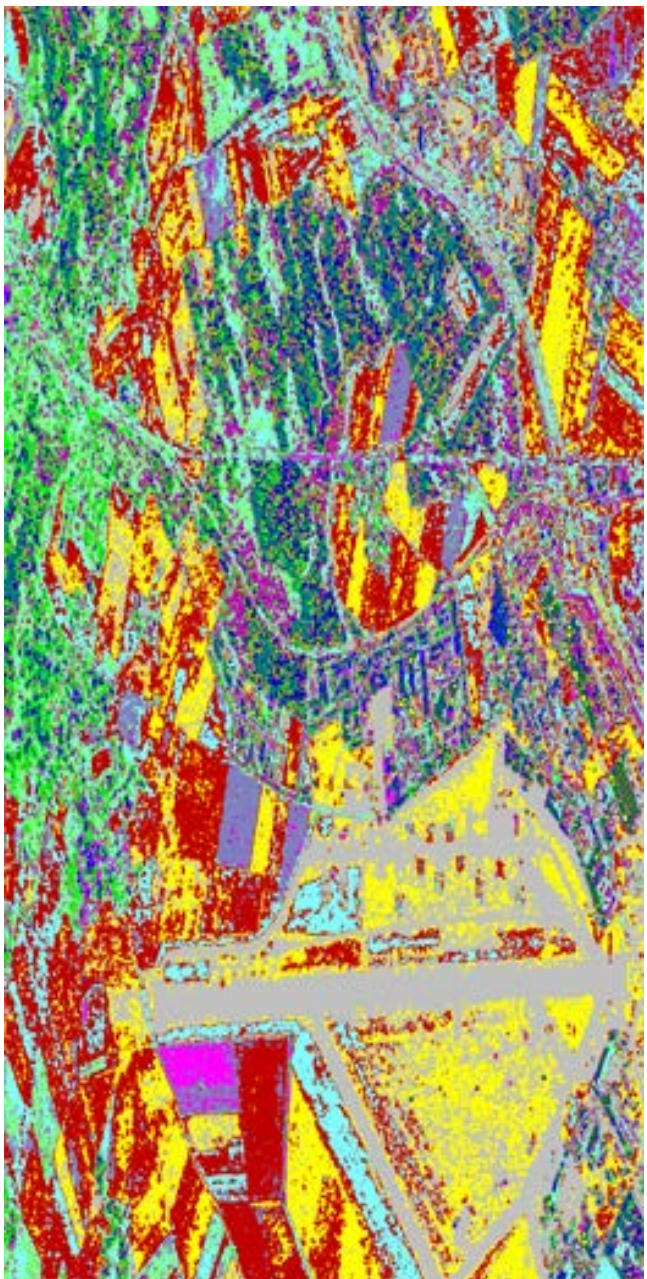
H/A/ α Wishart Classifier



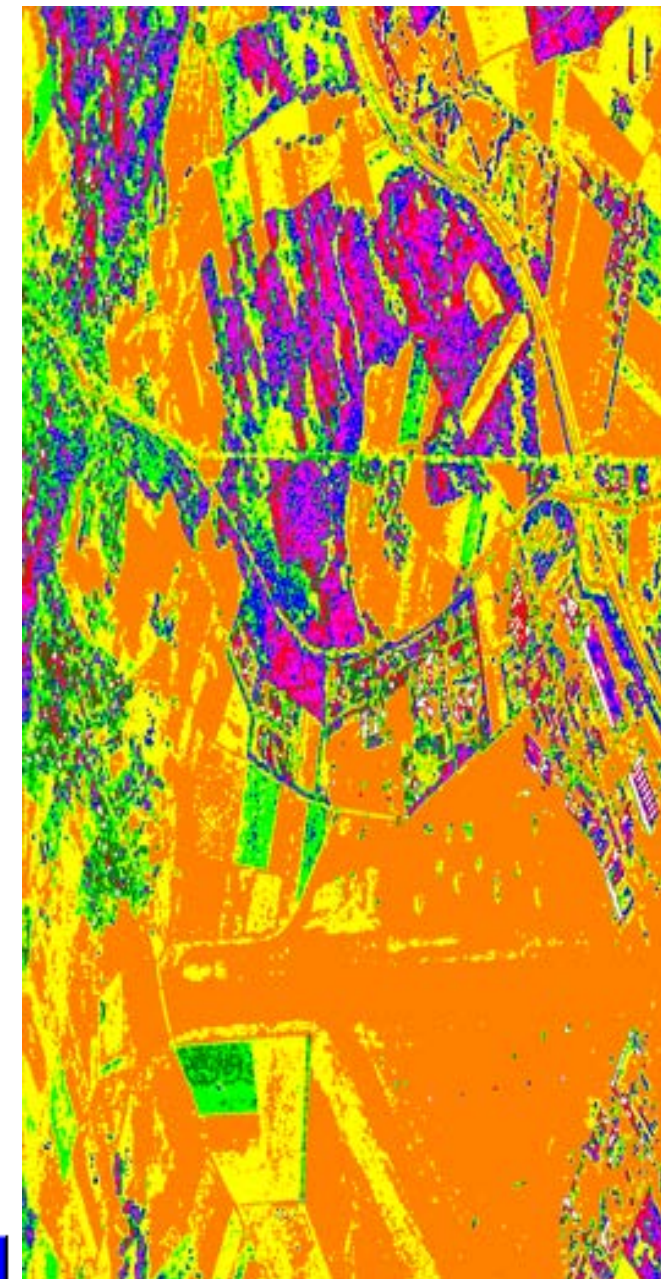
|Shh-Svv| 2|Shv| | Shh +Svv|



H/A/ α Wishart Classifier



H/A/ α Wishart Classifier



H/ α Wishart Classifier



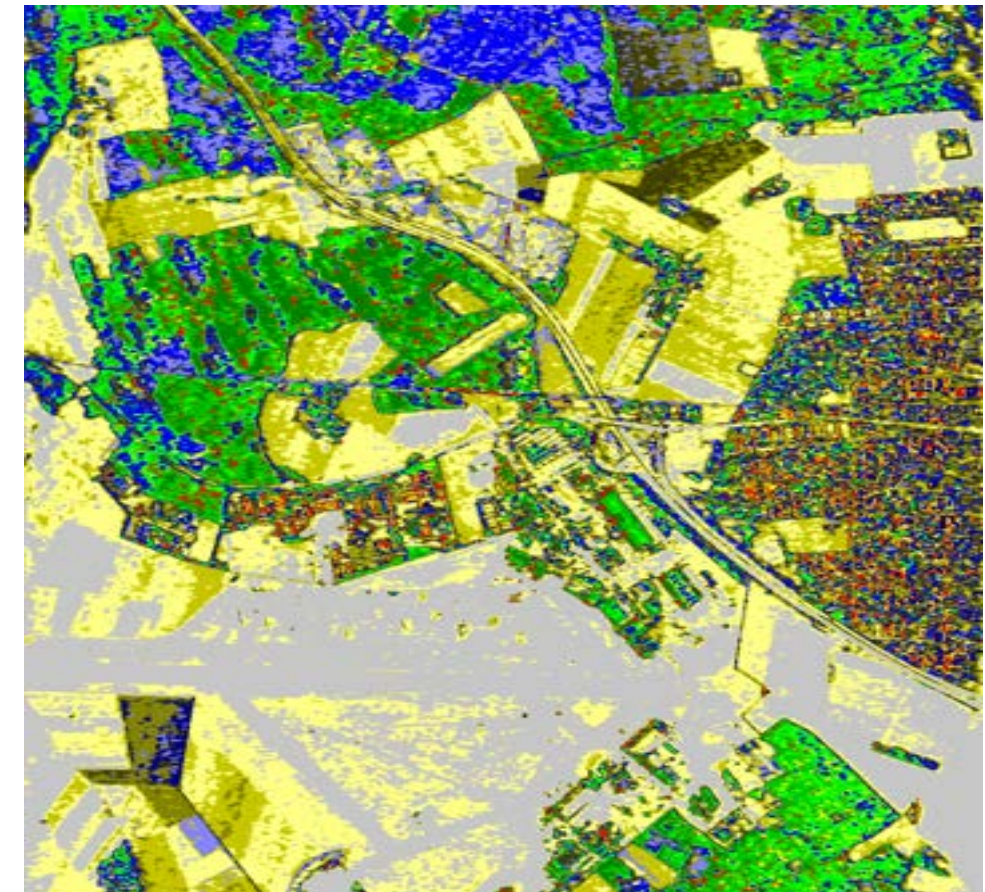
H/A/ α Wishart Classifier



|HH+VV|

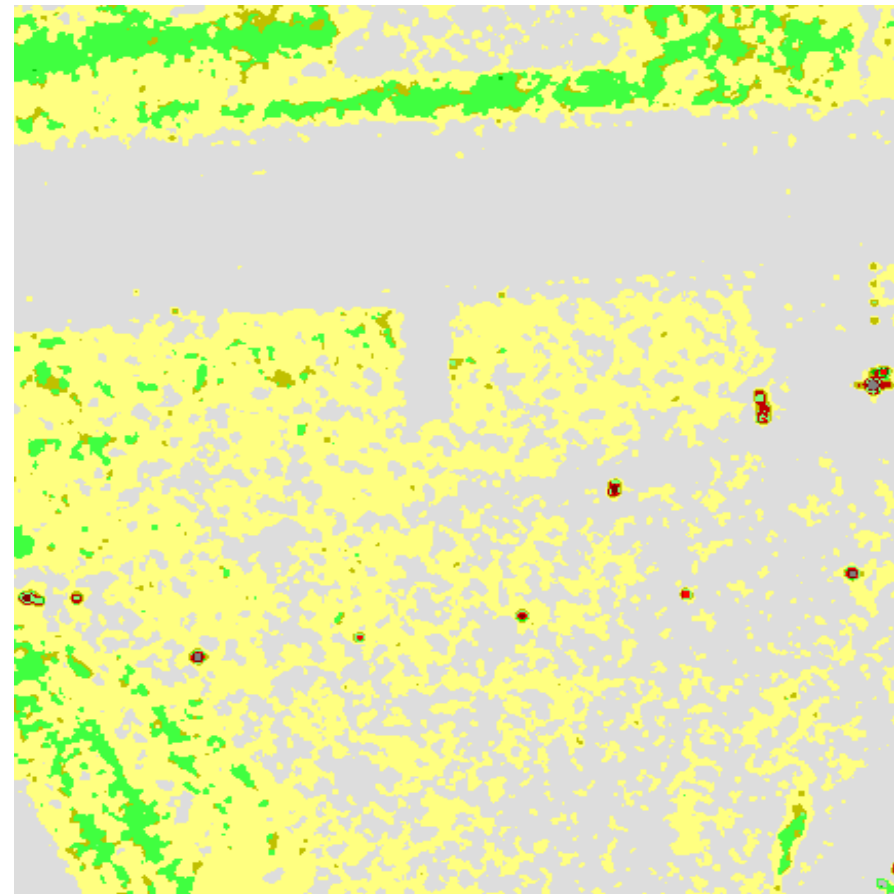
|HV|

|HH-VV|



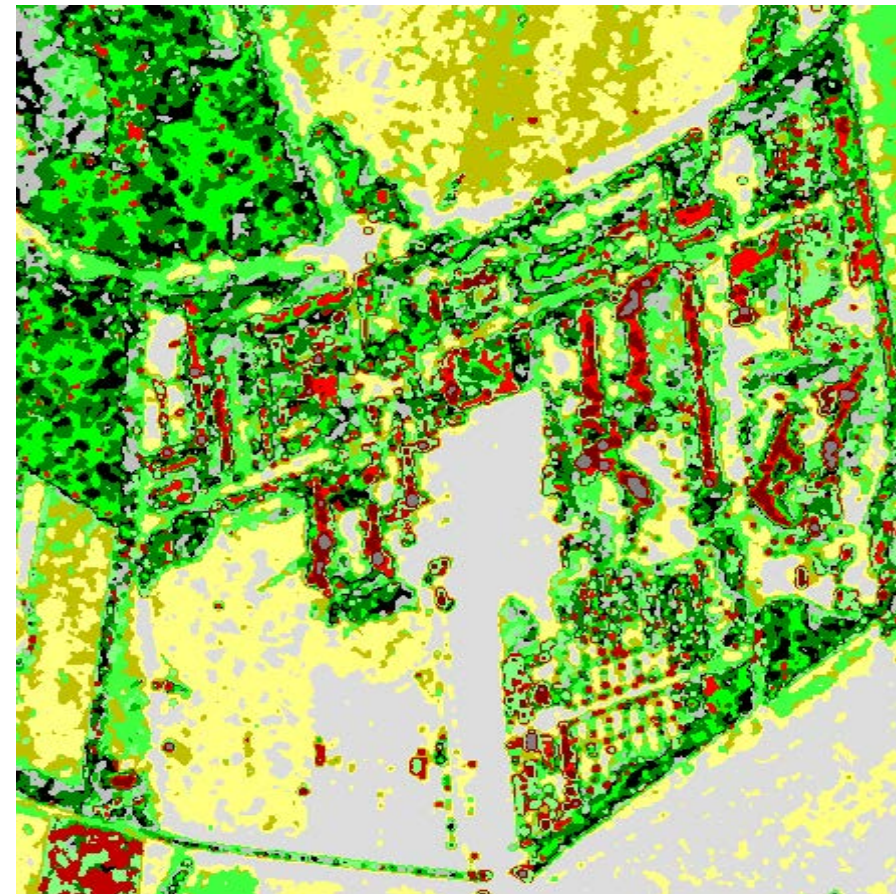
C1	C2	C3	C4	C5	C6	C7	C8
C9	C10	C11	C12	C13	C14	C15	C16

H/A/ α Wishart Classifier



C1	C2	C3	C4	C5	C6	C7	C8
C9	C10	C11	C12	C13	C14	C15	C16

H/A/ α Wishart Classifier



C1	C2	C3	C4	C5	C6	C7	C8
C9	C10	C11	C12	C13	C14	C15	C16

H/A/ α Wishart Classifier

SAN FRANCISCO BAY JPL - AIRSAR L-band 1988

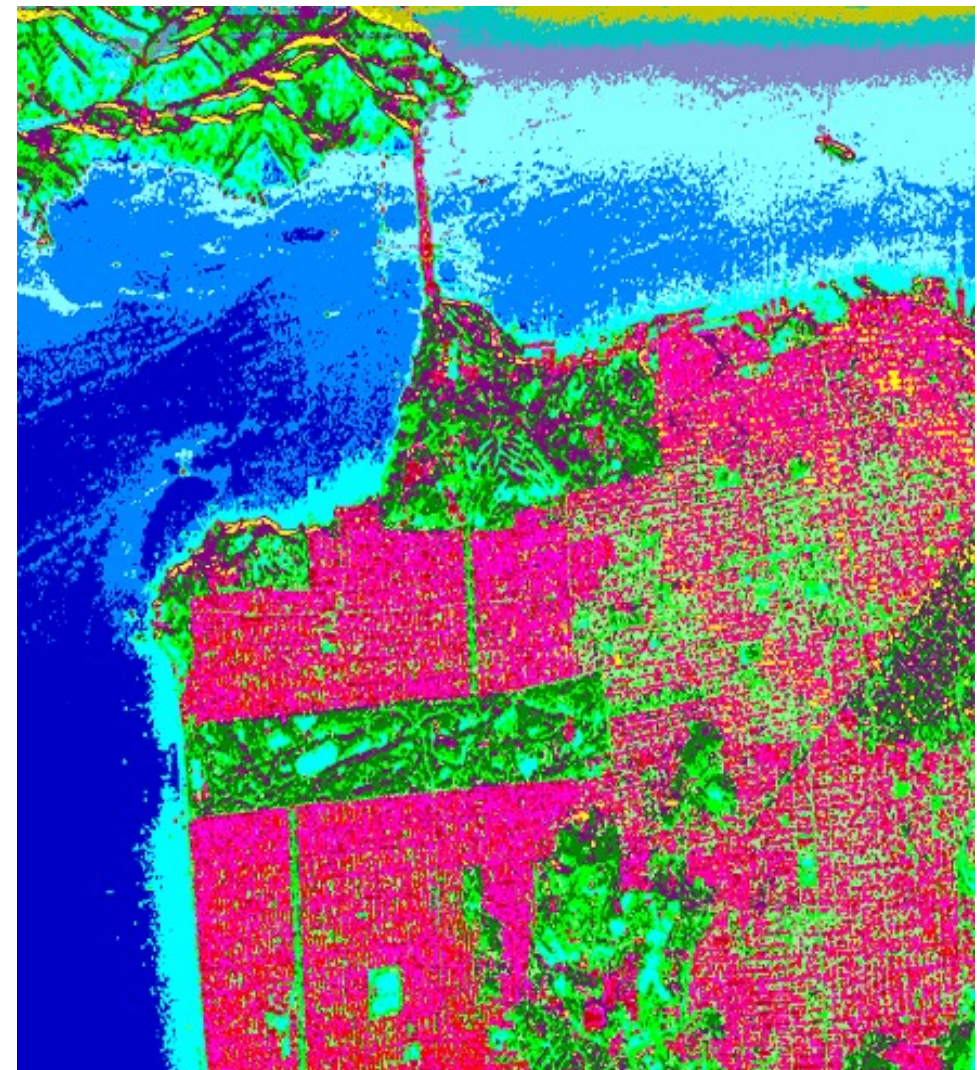


|HH+VV|

|HV|

|HH-VV|

4th ITERATION

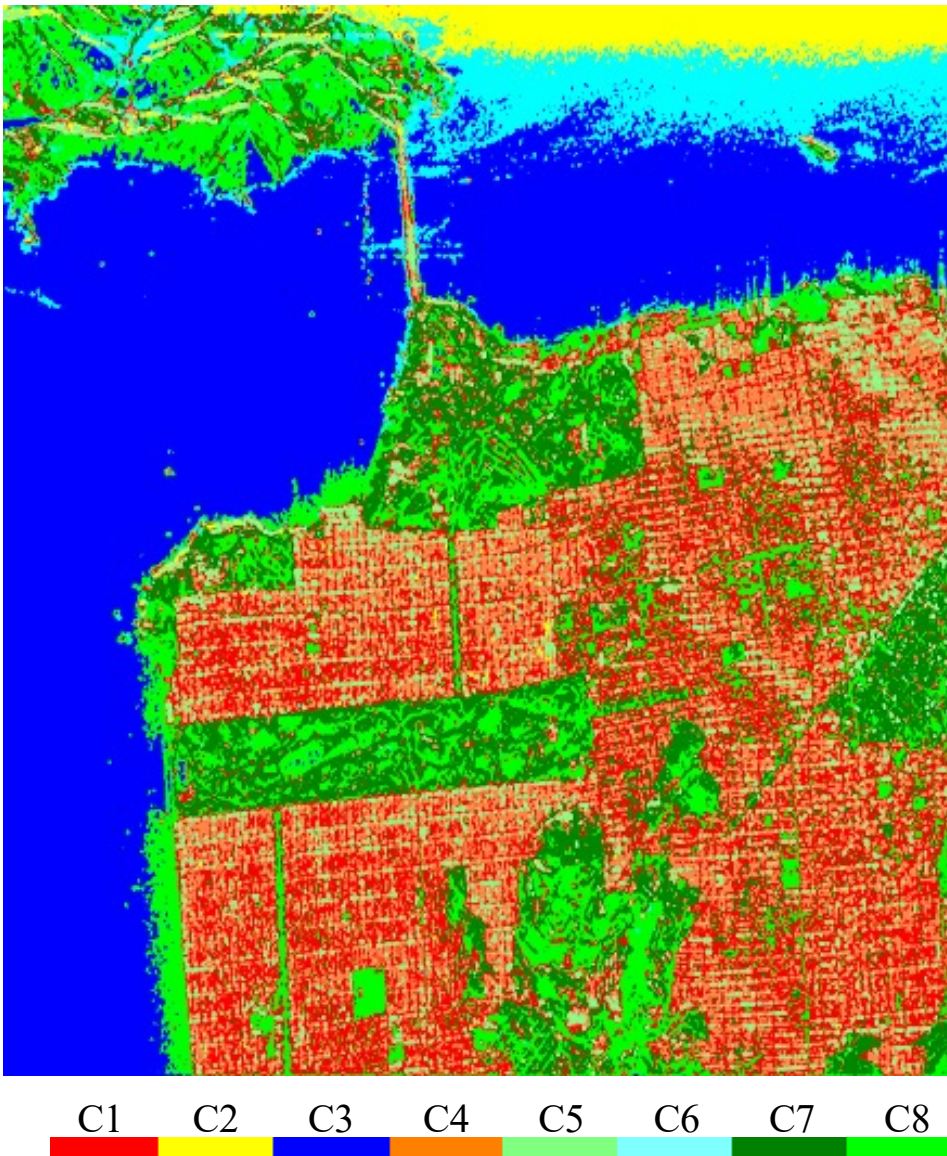


C1 C2 C3 C4 C5 C6 C7 C8

C9 C10 C11 C12 C13 C14 C15 C16

H/A/ α Wishart Classifier

H / $\underline{\alpha}$ and WISHART CLASSIFIER



H / A / $\underline{\alpha}$ and WISHART CLASSIFIER

